SIMPLE CONVERGENCE PROOF OF ADAM FROM A SIGN-LIKE DESCENT PERSPECTIVE

Anonymous authors
Paper under double-blind review

ABSTRACT

Adam is widely recognized as one of the most effective optimizers for training deep neural networks (DNNs). Despite its remarkable empirical success, its theoretical convergence analysis remains unsatisfactory. Existing works predominantly interpret Adam as a preconditioned stochastic gradient descent with momentum (SGDM), formulated as $\boldsymbol{x}_{t+1} = \boldsymbol{x}_t - \frac{\gamma}{\sqrt{\boldsymbol{v}_t}+\epsilon} \circ \boldsymbol{m}_t$. This perspective necessitates strong assumptions and intricate techniques, resulting in lengthy and opaque convergence proofs that are difficult to verify and extend. While many prior works have treated Adam as a sign-like optimizer to interpret its practical advantages, we are the first to formally provide a convergence proof for Adam from the perspective of sign-like descent, expressed as $\boldsymbol{x}_{t+1} = \boldsymbol{x}_t - \gamma \frac{|\boldsymbol{m}_t|}{\sqrt{\boldsymbol{v}_t}+\epsilon} \circ \mathrm{Sign}(\boldsymbol{m}_t)$. This reformulation significantly simplifies the convergence analysis. For the first time, with some mild conditions, we prove that Adam achieves the optimal rate of $\mathcal{O}(\frac{1}{T^{1/4}})$ rather than the previous $\mathcal{O}\left(\frac{\ln T}{T^{1/4}}\right)$ under weak assumptions of the generalized p-affine variance and (L_0, L_1, q)-smoothness, without dependence on the model dimensionality or the numerical stability parameter ϵ. Additionally, our theoretical analysis provides new insights into the role of momentum as a key factor ensuring convergence and offers practical guidelines for tuning learning rates in Adam, further bridging the gap between theory and practice.

1 INTRODUCTION

Currently, Adam (Kingma & Ba, 2015) has emerged as the predominant optimizer for training Transformers (Vaswani et al., 2017), particularly for state-of-the-art large language models (LLMs) (Brown et al., 2020; Chowdhery et al., 2023; Touvron et al., 2023a) and large vision models (Radford et al., 2021; Kirillov et al., 2023). Notably, Adam's influence extends beyond Transformers to modern convolutional neural networks (CNNs), such as ConvNeXt (Liu et al., 2022; Woo et al., 2023), where it has become the de facto choice for optimization. This is despite the traditional preference for stochastic gradient descent (SGD) (Krizhevsky et al., 2017; He et al., 2016), which was historically considered more suitable for CNN training.

However, the theoretical convergence analysis of Adam lags behind its significant practical success. The original proof in (Kingma & Ba, 2015) was based on the convexity of the objective function but was later found to be flawed (Reddi et al., 2018). To address this, AMSGrad, a fixed variant of Adam, was proposed, but its theoretical analysis still relied on the convexity assumption. Chen et al. (2018) were the first to theoretically demonstrate that a class of Adam-type optimizers, including AMSGrad and AdaFom, converge to stationary solutions for non-convex problems. Subsequently, Défossez et al. (2020) provided a simplified proof analyzing the convergence rates of vanilla Adam and Adagrad. However, their analysis required $\beta_1 < \beta_2$ and depended on the model dimensionality d. Chen et al. (2022) introduced practical, easy-to-check conditions to ensure the global convergence of Adam, but their proved convergence rate also heavily

Table 1: Comparison of different convergence proofs for Adam. "FCT" refers to the full corrective term. "Conv. Rate" denotes the convergence rate for approaching stationary points (*i.e.*, $\|\nabla F(\boldsymbol{x}_T)\|_2 \to 0$). T represents the number of iterations, E the number of epochs, d the model dimensionality, n the total number of samples, and ϵ the numerical stability parameter.

References	FCT	Noise Condition	Smooth Condition	Coeff. Condition	Conv. Rate
(Chen et al., 2018)	No	Bounded Grad.	L-Smooth	$\beta_{1_t} \leq \beta_1$, $\beta_{2_t} = 1 - \frac{1}{t}$	$\mathcal{O}\left(\frac{d^{1/2}\epsilon^{-1}\ln T}{T^{1/4}}\right)$
(Défossez et al., 2020)	No	Bounded Grad.	L-Smooth	$\beta_2 < \beta_1$, $\beta_2 = 1 - \frac{1}{T}$	$\mathcal{O}\left(\frac{d^{1/2}\ln(\epsilon^{-1}T)}{T^{1/4}}\right)$
(Chen et al., 2022)	No	Bounded Grad.	L-Smooth	$\boldsymbol{\beta_{2_t} < \sqrt{\beta_1}}$, $\beta_{2_t} = 1 - \frac{1}{t}$	$\mathcal{O}\left(\frac{d^{3/4}\ln\epsilon^{-1}\ln T}{T^{1/4}}\right)$
(Zhang et al., 2022)	No	Affine Var.	L-Smooth	$\boldsymbol{\beta_2 < \sqrt{\beta_1}}$, $\beta_2 = 1 - \mathcal{O}(\frac{1}{n^3})$	$\mathcal{O}\left(\frac{n^{1/2}d^{3/4}\ln E}{E^{1/4}}\right)$
(Wang et al., 2023c)	No	Bounded Var.	(L_0, L_1)-Smooth	$\boldsymbol{\beta_2 < \sqrt{\beta_1}}$, $\beta_2 = 1 - \mathcal{O}(\frac{1}{T})$	$\mathcal{O}\left(\frac{n^{1/2}d^{1/2}\ln E}{E^{1/4}}\right)$
(Li et al., 2023)	Yes	sub-Gaussian Var.	**Generalized (L_0, L_1, q)-Smooth**	$\boldsymbol{\beta_2 = 1 - \mathcal{O}(\frac{1}{T^{1/2}})}$	$\mathcal{O}\left(\frac{\epsilon^{-2}\ln T}{T^{1/4}}\right)$
(Hong & Lin, 2025)	Yes	Affine Var.	**Generalized (L_0, L_1, q)-Smooth**	$\beta_2 < \beta_1$, $\beta_2 = 1 - \mathcal{O}(\frac{1}{T})$	$\mathcal{O}\left(\frac{d\ln(\epsilon^{-1}T)}{T^{1/4}}\right)$
Corollary 3 [1]	Yes	**Generalized p-Affine Var.**	**Generalized (L_0, L_1, q)-Smooth**	$\boldsymbol{\beta_2 < \sqrt{\beta_1}}$, $\boldsymbol{\beta_2 = 1 - \mathcal{O}(\frac{1}{T^{3/4}})}$	$\boldsymbol{\mathcal{O}\left(\frac{1}{T^{1/4}}\right)}$

1. Compared to previous works, in Theorem 3.1 we establish the convergence of vanilla Adam under the weaker assumptions of generalized p-affine variance and (L_0, L_1, q)-smoothness (see Section 2 for definitions). Furthermore, we are the first to prove that Adam achieves the optimal convergence rate of $O(\frac{1}{T^{1/4}})$ in a dimension-free and ϵ-independent manner, improving upon the previous rate of $\mathcal{O}\left(\ln T/T^{1/4}\right)$. Note that our primary convergence result (Theorem 3.1) requires Conditions 1-3, while Theorem B.6 in the appendix provides a weaker result without them.

relied on the model dimensionality d. Notably, the analyses in (Chen et al., 2018; Défossez et al., 2020; Chen et al., 2022) all assumed bounded stochastic gradients. Later, Zhang et al. (2022) provided a theoretical proof for random-reshuffling Adam under the weaker affine variance assumption. However, this proof achieved a slower convergence rate with an epoch-complexity bound and relies on the total number of samples. Additionally, these works assumed the conventional uniformly bounded smoothness condition, *i.e.*, the L-smoothness condition. Recent studies, however, have shown that the L-smoothness assumption is inadequate for optimizing complex DNNs such as LSTMs and Transformers (Zhang et al., 2019; Crawshaw et al., 2022). Instead, it should be relaxed to the non-uniform (L_0, L_1)-smoothness condition (see Section 2 for details). Recently, Wang et al. (2023c) analyzed random-reshuffling Adam under the (L_0, L_1)-smoothness assumption, but their theoretical convergence rate was still based on epoch complexity and depended on the total number of samples. Li et al. (2023) demonstrated that Adam provably converges to stationary points with the optimal rate under generalized (L_0, L_1, q)-smoothness. However, this bound heavily relied on a large ϵ, making Adam behave similarly to SGD and losing its adaptive properties. Most recently, Hong & Lin (2025) established the convergence rate of a simplified Adam under both the affine variance and the generalized (L_0, L_1, q)-smoothness assumptions. However, their results still heavily depended on the model dimensionality. A detailed comparison of these convergence analyses for Adam is provided in Table 1.

All existing theoretical convergence proofs for Adam are path-dependent, treating Adam as a preconditioned SGD with momentum, as initially described in (Kingma & Ba, 2015), *i.e.*,$\boldsymbol{x}_{t+1} = \boldsymbol{x}_t - \frac{\gamma}{\sqrt{\boldsymbol{v}_t}+\epsilon} \circ \boldsymbol{m}_t$ where $\sqrt{\boldsymbol{v}_t} + \epsilon$ serves to precondition $\boldsymbol{m}_t$, introducing an effective learning rate of $\frac{\gamma}{\sqrt{\boldsymbol{v}_t}+\epsilon}$. This preconditioned formulation not only requires strong assumptions and intricate techniques for theoretical convergence analysis but also leads to proofs that are complex, lengthy, and difficult to verify or extend. Additionally, such theoretical analyses provide limited insights for practical optimization with Adam or for further enhancing the algorithm.

On the other hand, recent empirical evidence suggests that Adam's effectiveness may primarily stem from its sign-like property Balles & Hennig (2018). Kunstner et al. (2023) empirically demonstrates that sign descent with momentum achieves performance comparable to Adam when training Transformers, albeit without comprehensive analytical justification. Similarly, Chen et al. (2023b) employs an AutoML approach to discover a highly effective optimizer, Lion, which resembles signSGD with momentum and outperforms Adam across various DNN models. Kunstner et al. (2024) observed that Adam's superior performance on language models can be attributed to its sign-like property, which is particularly advantageous in addressing heavy-tailed class imbalance. Recently, Muon Jordan et al. (2024), an extended matrix-sign optimizer, has demonstrated significant potential for training DNNs Liu et al. (2025); Shah et al. (2025). However, no existing theoretical convergence proof for Adam considers its resemblance to sign descent, leaving its efficacy unexplained.

To address the aforementioned issues, we treat Adam as a stochastic sign-like descent optimizer to analyze its convergence. Specifically, we reformulate Adam as: $\boldsymbol{x}_{t+1} = \boldsymbol{x}_t - \gamma \frac{|\boldsymbol{m}_t|}{\sqrt{\boldsymbol{v}_t}+\epsilon} \circ \mathrm{Sign}(\boldsymbol{m}_t)$ where we take $\frac{|\boldsymbol{m}_t|}{\sqrt{\boldsymbol{v}_t}+\epsilon}$ as a single random variable. This reformulation not only completely circumvents the aforementioned challenges but also simplifies the proof process. Moreover, the provable convergence rate of the gradient norm in expectation achieves the optimal rate under the weak assumptions of non-uniform smoothness and affine variance noise without dependency on the model dimensionality d and the numerical-stability parameter ϵ. Additionally, this theoretical analysis enhances our understanding of the foundations underlying Adam's success. It sheds light on why momentum improves convergence, and how to better tune hyperparameters.

Our contributions are summarized as follow:

- We pioneer the establishment of a theoretical convergence proof for vanilla Adam from the perspective of sign-like descent. This approach circumvents the intractable challenges of preconditioned settings and significantly simplifies the proof process.
- We are the first to prove that vanilla Adam achieves the convergence rate of $\mathcal{O}(\frac{1}{T^{1/4}})$, compared to the previous $\mathcal{O}\left(\frac{\ln T}{T^{1/4}}\right)$, under the weak assumptions of generalized p-affine noise and (L_0, L_1, q)-smoothness along with some mild condidtions, without reliance on the model dimensionality or the numerical stability parameter ϵ.
- Our theoretical convergence analysis provides the insight into the significance of momentum and provides guidance on tuning the learning rate in Adam.

2 Preliminary

2.1 Notation

In this paper, the optimizer aims to minimize the empirical risk loss of a model on a dataset, *i.e.*,

$$\min_{\boldsymbol{x}\in\mathbb{R}^d} F(\boldsymbol{x}) = \mathbb{E}_{\zeta\sim\mathcal{D}}[f(\boldsymbol{x};\zeta)] = \frac{1}{n}\sum_{i=1}^{n} f(\boldsymbol{x};\omega_i), \tag{1}$$

where $\boldsymbol{x} \in \mathbb{R}^d$ and ζ are independently and identically sampled from the dataset $\{\omega_i : \omega_i \in \mathcal{D}, 1 \le i \le n\}$. For simplicity, we sometimes use $\boldsymbol{g} = \nabla f(\boldsymbol{x};\zeta)$.

As shown in Table 1, the previous studies (Chen et al., 2018; Défossez et al., 2020; Zhang et al., 2022; Wang et al., 2023c) have omitted the bias correction in Line 6-7 of Algorithm 1 when analyzing the convergence rate, while we will provide the theoretical analysis of vanilla Adam with bias correction.

Algorithm 1. Adam

Input: the momentum $\boldsymbol{m}_0 = 0$, $\boldsymbol{v}_0 = 0$, the numerical stable constant ϵ, the exponential moving average coefficient β_1 and β_2, and the learning rate γ.
for $t = 1, ..., T$ **do**
  Randomly sample data and compute the gradient: $\boldsymbol{g}_t \leftarrow \nabla f(\boldsymbol{x}_t; \zeta_t)$
  Update the momentum $\boldsymbol{m}_t$: $\boldsymbol{m}_t \leftarrow \beta_1 \boldsymbol{m}_{t-1} + (1-\beta_1)\boldsymbol{g}_t$
  Update the momentum $\boldsymbol{v}$: $\boldsymbol{v}_t \leftarrow \beta_2 \boldsymbol{v}_{t-1} + (1-\beta_2)\boldsymbol{g}_t^2$
  Compute the bias corrected $\hat{\boldsymbol{m}}_t$: $\hat{\boldsymbol{m}}_t \leftarrow \frac{\boldsymbol{m}_t}{1-\beta_1^t}$
  Compute the bias corrected $\hat{\boldsymbol{v}}_t$: $\hat{\boldsymbol{v}}_t \leftarrow \frac{\boldsymbol{v}_t}{1-\beta_2^t}$
  Update the model parameter: $\boldsymbol{x}_{t+1} \leftarrow \boldsymbol{x}_t - \gamma \frac{\hat{\boldsymbol{m}}_t}{\sqrt{\hat{\boldsymbol{v}}_t}+\epsilon}$
end for

2.2 Details of Adam

To facilitate the analysis of Adam, we provide the details of Adam in Algorithm 1.

2.3 Assumptions and Conditions

To analyze the convergence rate of Adam, we list the main assumption as follows.

Assumption A [Bounded Infimum]. *There exists a constant $F^* > -\infty$, and the objective function follows $F(\boldsymbol{x}) \geq F^*$ for any $\boldsymbol{x} \in \mathbb{R}^d$.*

Assumption B.1 [L-Smoothness] *There exists a constants $L \geq 0$, and then for any $\boldsymbol{x}, \boldsymbol{y} \in \mathbb{R}^d$, the gradient of the objective function follows*

$$\|\nabla F(\boldsymbol{y}) - \nabla F(\boldsymbol{x})\|_2 \leq L\|\boldsymbol{x} - \boldsymbol{y}\|_2. \tag{2}$$

Assumption B.2 [(L_0, L_1)-Smoothness] *There exist constants $L_0, L_1 \geq 0$, and then for any $\boldsymbol{x}, \boldsymbol{y} \in \mathbb{R}^d$, the gradient of the objective function follows*

$$\|\nabla F(\boldsymbol{y}) - \nabla F(\boldsymbol{x})\|_2 \leq (L_0 + L_1\|\nabla F(\boldsymbol{x})\|_2)\|\boldsymbol{x} - \boldsymbol{y}\|_2. \tag{3}$$

Assumption B.3 [(L_0, L_1, q)-Smoothness] *There exist constants $L_0, L_1 > 0$ and $0 \leq q \leq 1$, and then for any $\boldsymbol{x}, \boldsymbol{y} \in \mathbb{R}^d$, the gradient of the objective function follows*

$$\|\nabla F(\boldsymbol{y}) - \nabla F(\boldsymbol{x})\|_2 \leq (L_0 + L_1\|\nabla F(\boldsymbol{x})\|_2^q)\|\boldsymbol{x} - \boldsymbol{y}\|_2. \tag{4}$$

When $q = 1$, the generalized (L_0, L_1, q)-smoothness (Assumption B.3) is reduced to the (L_0, L_1)-smoothness (Assumption B.2). When $L_1 = 0$ or $q = 0$, the generalized (L_0, L_1, q)-smoothness (Assumption B.3) is reduced to the standard L-smoothness (Assumption B.1). (L_0, L_1)-smoothness was originally defined in (Zhang et al., 2019) as a bound on the second-order Hessian function. Following Zhang et al. (2020), we reformulate the (L_0, L_1)-smoothness as an affine form of the gradient norm for first-order differentiable functions. Subsequently, Li et al. (2023) first introduced the generalized (L_0, L_1, q)-smoothness to analyze the convergence of Adam, followed by Wang et al. (2024) and Hong & Lin (2025).

Assumption C.1 [Bounded Variance]. *There exists a positive constant $\sigma_0 > 0$, and then for any $\boldsymbol{x}_t \in \mathbb{R}^d$, the noisy gradient of the objective function obeys*

$$\mathbb{E}[\nabla f(\boldsymbol{x}; \zeta)] = \nabla F(\boldsymbol{x}), \quad \mathbb{E}[\|\nabla f(\boldsymbol{x}; \zeta) - \nabla F(\boldsymbol{x})\|_2^2] \leq \sigma_0^2. \tag{5}$$

Assumption C.2 [Affine Variance]. *There exist constants $\sigma_0, \sigma_1 \geq 0$, and then for $\boldsymbol{x} \in \mathbb{R}^d$, the noisy gradient of the objective function obeys*

$$\mathbb{E}[\nabla f(\boldsymbol{x}; \zeta_t)] = \nabla F(\boldsymbol{x}), \quad \mathbb{E}[\|\nabla f(\boldsymbol{x}; \zeta) - \nabla F(\boldsymbol{x})\|_2^2] \leq \sigma_0^2 + \sigma_1^2\|\nabla F(\boldsymbol{x})\|_2^2. \tag{6}$$

Assumption C.3 [p-Affine Variance]. *There exist constants $\sigma_0, \sigma_1 \geq 0$ and $0 \leq p \leq 2$, and then $\boldsymbol{x} \in \mathbb{R}^d$ at any time, the noisy gradient of the objective function obeys*

$$\mathbb{E}[\nabla f(\boldsymbol{x}; \zeta_t)] = \nabla F(\boldsymbol{x}), \quad \mathbb{E}[\|\nabla f(\boldsymbol{x}; \zeta) - \nabla F(\boldsymbol{x})\|_2^2] \leq \sigma_0^2 + \sigma_1^2 \|\nabla F(\boldsymbol{x})\|_2^p. \tag{7}$$

When $p = 2$, the p-affine variance (Assumption C.3) is reduced to the affine variance (Assumption C.2). When $\sigma_1 = 0$ or $p = 0$, the p-affine variance (Assumption C.3) is reduced to the bounded variance (Assumption C.1). The affine variance (Assumption C.2) was originally studied in (Bertsekas & Tsitsiklis, 2000) to analyze the convergence behavior of SGD. It was later applied to analyze AdaGrad (Faw et al., 2022; Wang et al., 2023a) and a simplified Adam (Wang et al., 2024).

To the best of our knowledge, Assumption B.3 and Assumption C.3 are the weakest assumptions for analyzing the convergence of Adam among the existing literatures.

In addition, we also list the following required conditions.

Condition 1 *At any t-th iteration in Algorithm 1, the gradients satisfy $\sqrt{\frac{1}{T}\sum_{t=1}^{T}\|\nabla F(\boldsymbol{x}_t)\|_2^2} \leq \frac{C_0}{T}\sum_{t=1}^{T}\|\nabla F(\boldsymbol{x}_t)\|_2$ with $1 \leq C_0 \ll \sqrt{T}$.*

Condition 2 *At any t-th iteration in Algorithm 1, the coordinates of the update in Adam , i.e., $u_t = \frac{|\boldsymbol{m}_t^{(j)}|}{\sqrt{\boldsymbol{v}_t^{(j)}}+\epsilon}(j \in [d])$, are independently and identically distributed (i.i.d), and the mean update is bounded away from zero, $\bar{u}_t = \frac{1}{d}\sum_{j=1}^{d}\frac{|\boldsymbol{m}_t^{(j)}|}{\sqrt{\boldsymbol{v}_t^{(j)}}+\epsilon} > 0$.*

Condition 3 *At any t-th iteration in Algorithm 1, the gradient satisfies $\|\nabla F(\boldsymbol{x}_t)\|_1 = \frac{\sqrt{d}}{C_1}\|\nabla F(\boldsymbol{x}_t)\|_2$ with $1 \leq C_1 \ll \sqrt{d}$.*

Condition 1 is easily satisfied when the gradients $\|\nabla F(\boldsymbol{x}_t)\|_2$ decrease at a rate of $\Theta\left(\frac{1}{t^\alpha}\right)$ for all $0 < \alpha < \frac{1}{2}$, and the number of iterations is sufficiently large. We summarize this in the following proposition.

Proposition 1 *If $\|\nabla F(\boldsymbol{x}_t)\|_2$ decreases at the rate of $\Theta\left(\frac{1}{t^\alpha}\right)$ for $0 \leq \alpha < \frac{1}{2}$ and $T \geq 8$, then it holds that*

$$\frac{\frac{1}{T}\sum_{t=1}^{T}\|\nabla F(\boldsymbol{x}_t)\|_2^2}{\left(\frac{1}{T}\sum_{t=1}^{T}\|\nabla F(\boldsymbol{x}_t)\|_2\right)^2} \leq \mathcal{O}\left(\frac{2(1-\alpha)^2}{1-2\alpha}\right). \tag{8}$$

Arjevani et al. (2023) has demonstrated that the optimal convergence rate of $\|\nabla F(\boldsymbol{x}_t)\|_2$ in non-convex stochastic optimization is $\mathcal{O}\left(\frac{1}{T^{1/4}}\right)$, which lies in the range $[0, \frac{1}{2})$. We choose a sufficiently large T in practice, meaning T is greatly larger than $\frac{2(1-\alpha)^2}{1-2\alpha}$. Therefore, Condition 1 commonly holds in practice.

Condition 2 commonly holds in practice, and we empirically validated it in our experiments, as shown in Figure 1. Specifically, we employed Adam to train ResNet-50 on ImageNet and GPT-2 (350M) on OpenWebText. During training, we recorded $\boldsymbol{m}_t^{(j)}/\sqrt{\boldsymbol{v}_t^{(j)}}$ for each coordinate in certain layers. To verify whether $|\boldsymbol{m}_t^{(j)}|/\sqrt{\boldsymbol{v}_t^{(j)}}$ for each coordinate is drawn from the same distribution, we used the two-sample Kolmogorov-Smirnov (KS) test. In this test, two groups of 10,000 samples were uniformly drawn from all coordinates of the layer, and these groups were used to run the two-sample KS test. We repeated this procedure 1,000 times and reported the mean p-value. As illustrated in Figure 1, the mean p-value is significantly larger than the significance level of 0.05, strongly suggesting that $\boldsymbol{m}_t^{(j)}/\sqrt{\boldsymbol{v}_t^{(j)}}$ for each coordinate in the layers is independently drawn from an identical distribution. It can also be observed that the mean value of $\hat{\boldsymbol{m}}_t^{(j)}/(\sqrt{\hat{\boldsymbol{v}}_t^{(j)}} + 10^{-8})$ stays almost stable and remains bounded away from zero during training.

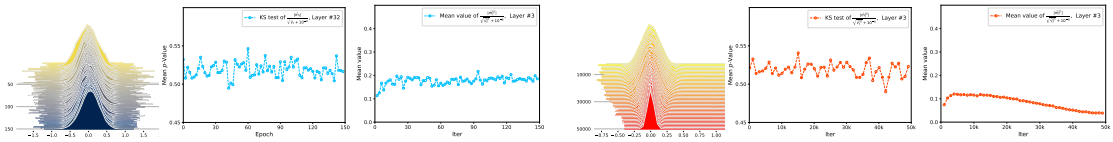

(a) ResNet-50, Layer#32 (b) GPT-2 (350M), Layer#3

Figure 1: The distribution, the two-sample Kolmogorov-Smirnov test and the mean value of $\hat{\boldsymbol{m}}_t^{(j)}/(\sqrt{\hat{\boldsymbol{v}}_t^{(j)}}+10^{-8})$ across coordinates of (a) Layer#32.conv.weight in ResNet-50 during training with Adam on ImageNet for 150 epochs, and (b) Layer#3.self-attention.in-proj-weight in GPT-2 (350M) during training with Adam on OpenWebText for 5,000 iterations. In this test, two groups of 10,000 samples were uniformly drawn from all coordinates of the layer, and these groups were used to run the two-sample KS test. We repeated this procedure 1,000 times and reported the mean p-value. The p-values significantly exceed the 0.05 threshold, strongly indicating that the values of $\hat{\boldsymbol{m}}_t^{(j)}/(\sqrt{\hat{\boldsymbol{v}}_t^{(j)}}+10^{-8})$ are independently drawn from the identical distribution. It can also be observed that the mean value of $\hat{\boldsymbol{m}}_t^{(j)}/(\sqrt{\hat{\boldsymbol{v}}_t^{(j)}}+10^{-8})$ stays almost stable and remains bounded away from zero during training.

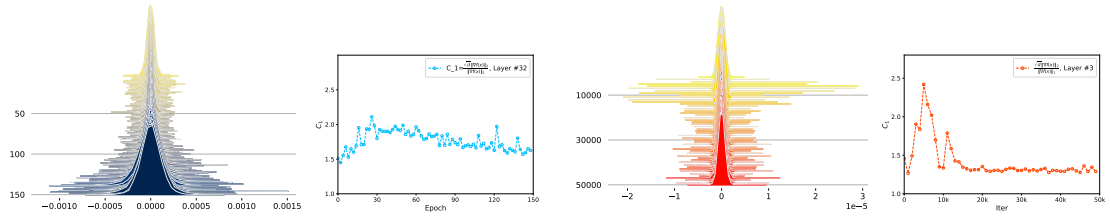

(a) ResNet-50, Layer#32 (b) GPT-2 (350M), Layer#3

Figure 2: The distribution and $C_1 = \frac{\sqrt{d}\|\nabla f(\boldsymbol{x}_t)\|_2}{\|\nabla f(\boldsymbol{x}_t)\|_1}$ for gradients across coordinates of (a) Layer#32.conv.weight in ResNet-50 during training with Adam on ImageNet for 150 epochs, and (b) Layer#3.self-attention.in-proj-weight in GPT-2 (350M) during training with Adam on OpenWebText for 50,000 iterations. Throughout training, C_1 remains consistently below 3, which is significantly smaller than $\sqrt{d}$, where d represents the number of coordinates in the layers.

Condition 3 commonly holds in practice, and we also empirically validated it in our experiments, as shown in Figure 2. Specifically, we employed Adam to train ResNet-50 on ImageNet and GPT-2 (350M) on OpenWebText. During training, we recorded the gradient $\nabla f(\boldsymbol{x}_t)$ for each coordinate in selected layers. Subsequently, we computed $C_1 = \frac{\sqrt{d}\|\nabla f(\boldsymbol{x}_t)\|_2}{\|\nabla f(\boldsymbol{x}_t)\|_1}$. As shown in Figure 2, C_1 consistently remains below 3 throughout training, which is significantly smaller than $\sqrt{d}$, where d represents the number of coordinates in the layers. This observation can be attributed to the fact that the coordinates of $\nabla f(\boldsymbol{x}_t)$ tend to be densely clustered during training, as also depicted in Figure 2.

3 Main Result

We first state the preliminary result in Theorem 2 under Assumptions A, B.3 and C.3. Then, we derive the more comprehensive convergence bound of Adam with Conditions 1, 2 and 3 in Corollary 3.

Theorem 2 *Let $\{x_t\}_{t=1}^T$ be generated by Algorithm 1. Suppose that Assumptions A, B.3, and C.3, along with Condition 1, hold. Define $u_t^{(j)} := |\boldsymbol{m}_t^{(j)}|/(\sqrt{\boldsymbol{v}_t^{(j)}}+\epsilon)$, $R := (1-\beta_1)/\sqrt{(1-\beta_2)(1-\frac{\beta_1^2}{\beta_2})}$, $\hat{L} := L_0 + (1-q)L_1$, and $\hat{\sigma} := \sigma_0 + \sqrt{\frac{2-p}{2}}$. Choose $\beta_1 < \sqrt{\beta_2}$. Then, it holds for any $T \in \mathbb{N}^+$,*

$$\frac{1}{T}\left(\sum_{t=1}^{T}\mathbb{E}[\|\boldsymbol{u}_t \circ \nabla F(\boldsymbol{x}_t)\|_1] - \left(\frac{\gamma R^2 dqL_1}{2} + 2C_0 R\sqrt{d}\sigma_1\sqrt{p(1-\beta_1)} + \frac{2\gamma R^2 dqL_1}{1-\beta_1}\right)\sum_{t=1}^{T}\mathbb{E}[\|\nabla F(\boldsymbol{x}_t)\|_2]\right) \tag{9}$$
$$\leq \frac{F(\boldsymbol{x}_1)-F^*}{\gamma T} + \frac{2R\sqrt{d}\,\|\nabla F(\boldsymbol{x}_1)\|_2}{T(1-\beta_1)} + 2\sqrt{1-\beta_1}R\sqrt{d}\hat{\sigma} + \frac{2\gamma R^2 d\hat{L}}{1-\beta_1} + \frac{\gamma R^2 d\hat{L}}{2}.$$

Corollary 3 *Let $\{x_t\}_{t=1}^T$ be generated by Algorithm 1. Suppose Assumptions A, B.3 and C.3, along Conditions 1,2 and 3, hold. Define $u_t := |\hat{\boldsymbol{m}}_t^{(j)}|/(\sqrt{\hat{\boldsymbol{v}}_t^{(j)}}+\epsilon)$, $R := {}^{1-\beta_1}/_{\sqrt{(1-\beta_2)(1-\beta_1^2/\beta_2)}}$, $\hat{L} := L_0 + (1-q)L_1$, and $\hat{\sigma} := \sigma_0 + \sqrt{\frac{2-p}{2}}$.*

Case 1: General Setting with no Access to Oracles

Choose $\gamma = \frac{C_2}{T^{3/4}d^{1/2}}$, $\beta_1 < \sqrt{\beta_2}$, $1-\beta_1 = \frac{C_3}{T^{1/2}}$, and $0 < \bar{v} \le \min_t \mathbb{E}[\boldsymbol{u}_t^{(j)}]$. Then, it holds for any $T \in \mathbb{N}^+$ and $T \ge (\frac{4C_1C_2R^2qL_1}{C_3\bar{v}} + \frac{4C_0C_1\sqrt{C_3}R\sigma_1\sqrt{p}}{\bar{v}} + (\frac{C_1C_2R^2qL_1}{\bar{v}})^{1/3})^4$,

$$\frac{1}{T}\sum_{t=1}^{T}\mathbb{E}[\|\nabla F(\boldsymbol{x}_t)\|_2] \le \frac{C_1}{\bar{v}}\left(\frac{2(F(\boldsymbol{x}_1)-F(\boldsymbol{x}^*))}{C_2T^{1/4}} + \frac{4R\|\nabla F(\boldsymbol{x}_1)\|_2}{C_3T^{1/2}} + \frac{4C_3R\hat{\sigma}}{T^{1/4}} + \frac{4C_2R^2\hat{L}}{C_3T^{1/4}} + \frac{C_2R^2\hat{L}}{T^{3/4}}\right). \tag{10}$$

Case 2: Lowest-Bound Setting with Access to Oracles

Choose $\hat{C}_2 = \frac{(F(\boldsymbol{x}_1)-F^*)^{3/4}}{2^{1/4}R\hat{\sigma}^{1/2}\hat{L}^{1/4}}$, $\hat{C}_3 = \frac{2^{1/2}\hat{L}^{1/2}(F(\boldsymbol{x}_1)-F^*)^{1/2}}{\hat{\sigma}}$, $\gamma = \frac{\hat{C}_2}{T^{3/4}d^{1/2}}$, $\beta_1 < \sqrt{\beta_2}$, $1-\beta_1 = \frac{\hat{C}_3}{T^{1/2}}$, and $0 < \bar{v} \le \min_t \mathbb{E}[\boldsymbol{u}_t^{(j)}]$. Then, for any $T \in \mathbb{N}^+$ and $T \ge (\frac{4C_1\hat{C}_2R^2qL_1}{\hat{C}_3\bar{v}} + \frac{4C_0C_1\sqrt{\hat{C}_3}R\sigma_1\sqrt{p}}{\bar{v}} + (\frac{C_1\hat{C}_2R^2qL_1}{\bar{v}})^{1/3})^4$, it reaches the lowest bound, i.e.,

$$\frac{1}{T}\sum_{t=1}^{T}\mathbb{E}[\|\nabla F(\boldsymbol{x}_t)\|_2] \le \frac{C_1}{\bar{v}}\left(\frac{512^{1/4}R\hat{\sigma}^{1/2}\hat{L}^{1/4}(F(\boldsymbol{x}_1)-F^*)^{1/4}}{T^{1/4}} + \frac{4R\|\nabla F(\boldsymbol{x}_1)\|_2}{\hat{C}_3T^{1/2}} + \frac{\hat{C}_2R^2\hat{L}}{T^{3/4}}\right). \tag{11}$$

We have some findings from Theorem 3 below.

Finding 1. To the best of our knowledge, we are the first to formally analyze Adam under the weak assumptions of generalized non-uniform (L_0, L_1, q)-smoothness (Assumption B.3) and p-affine variance (Assumption C.3). We also prove that $\frac{1}{T}\sum_{t=1}^{T}\mathbb{E}[\|\nabla F(\boldsymbol{x}_t)\|_2]$ for Adam achieves a tighter bound of $\mathcal{O}\left(\frac{1}{T^{1/4}}\right)$, compared to the previous $\mathcal{O}\left(\frac{\ln T}{T^{1/4}}\right)$ (Chen et al., 2018; Défossez et al., 2020; Chen et al., 2022; Li et al., 2023). Furthermore, earlier works demonstrated that Adam's convergence rates were dependent on the model dimensionality d and the numerical-stability ϵ (Chen et al., 2018; Défossez et al., 2020; Chen et al., 2022; Li et al., 2023), which makes them unsuitable to analyze large-scale LLM training. However, as shown in Corollary 3, we prove that Adam achieves dimension-free and ϵ-free convergence, similar to SGD (Bottou et al., 2018). Notably, previous studies required a learning rate of $\gamma = 1-\mathcal{O}(\frac{1}{T})$ to reach the optimal convergence rate of $\mathcal{O}\left(\frac{\ln T}{T^{1/4}}\right)$. This causes $\boldsymbol{v}_t$ to closely resemble a plain average of the past T squared gradients, reducing Adam almost to AdaGrad (Défossez et al., 2020). By contrast, we only require the learning rate to satisfy $\gamma = 1-\mathcal{O}(\frac{1}{T^{3/4}})$, which better aligns with Adam's original design.

Finding 2. The momentum coefficients β_1 and β_2 play a crucial role in Adam's convergence. As shown in Theorem 2, when $\beta_1 = \beta_2 = 0$, Adam reduces to signSGD, which converges at best to a bounded region where $\frac{1}{T}\sum_{t=1}^{T}\mathbb{E}[\|\nabla F(\boldsymbol{x}_t)\|_2] \le \mathcal{O}(\frac{1}{T^{1/4}} + \sigma_0)$. This result aligns with prior work (Bernstein et al., 2018). In contrast, sufficiently large values of β_1 and β_2 ensure Adam achieves the convergence rate of $\mathcal{O}(\frac{1}{T^{1/4}})$. For SGD, however, momentum has minimal impact on the optimal theoretical convergence rate, as both momentum-SGD and vanilla SGD converge at $\mathcal{O}(\frac{1}{T^{1/4}})$ (Bottou et al., 2018; Liu et al., 2020).

Finding 3. Case 2 in Corollary 3 states that Adam's learning rate must satisfy $\gamma = \mathcal{O}(\frac{1}{\sqrt{d}})$ to achieve the optimal convergence rate. This implies that, with fixed other hyperparameters, larger model sizes require smaller optimal learning rates. This observation has been empirically validated by practitioners training the

Llama family of models across different sizes (Touvron et al., 2023a;b; Dubey et al., 2024). Interestingly, a similar theoretical conclusion appears in the work on Maximal Update Parametrization (μP) (Yang et al., 2022).

4 Proof Sketch

In this section, we present the core ideas underlying the convergence proofs for Theorem 2 and Case 2 of Corollary 3. The proof ideas for Case 1 of Corollary 3 is similar, and thus, we omit the details for simplicity.

Our main contribution lies in opening up a new approach to proving the convergence of Adam. All existing theoretical convergence proofs follow a path-dependent approach, treating Adam as a preconditioned SGD with momentum, as originally presented in the Adam paper (Kingma & Ba, 2015). Specifically, the update rule is defined as: *i.e.*,$\boldsymbol{x}_t+1 = \boldsymbol{x}_t - \frac{\gamma_t}{\sqrt{\boldsymbol{v}_t}+\epsilon} \circ \boldsymbol{m}_t$, where $\sqrt{\boldsymbol{v}_t} + \epsilon$ is used to precondition $\boldsymbol{m}_t$, and the effective learning rate is $\frac{\gamma_t}{\sqrt{\boldsymbol{v}_t}+\epsilon}$. This approach, however, encounters two intractable issues: (i) the effective learning rate $\frac{\gamma_t}{\sqrt{\boldsymbol{v}_t}+\epsilon}$ is not necessarily monotone-decreasing, and (ii) the random variable $\boldsymbol{v}_t$ is not independent of $\boldsymbol{g}_t$ or $\boldsymbol{m}_t$. To address these challenges, the proofs in previous works became complicated, lengthy, and opaque, making them difficult to verify and extend. In contrast, we treat Adam as a whole stochastic sign-like descent algorithm, *i.e.*, $\boldsymbol{x}_{t+1} = \boldsymbol{x}_t - \gamma_t \frac{|\boldsymbol{m}_t|}{\sqrt{\boldsymbol{v}_t}+\epsilon} \circ \mathrm{Sign}(\boldsymbol{m}_t)$ where we consider the term $\frac{|\boldsymbol{m}_t|}{\sqrt{\boldsymbol{v}_t}+\epsilon}$ as a single random variable. This transformation not only circumvents the problems mentioned above but also simplifies the proof process. We now provide a sketch of the proof.

Under Assumption B.3, we obtain (details please refer to Lemma 1 in the Appendix):

$$\mathbb{E}[F(\boldsymbol{x}_{t+1})] \leq F(\boldsymbol{x}_t) + \mathbb{E}[\langle \nabla F(\boldsymbol{x}_t), \boldsymbol{x}_{t+1} - \boldsymbol{x}_t \rangle] + \frac{L_0 + L_1 \|\nabla F(\boldsymbol{x}_t)\|_2^q}{2} \mathbb{E}[\|\boldsymbol{x}_{t+1} - \boldsymbol{x}_t\|_2^2]. \tag{12}$$

Defining $\boldsymbol{u}_t := \frac{|\boldsymbol{m}_t|}{\sqrt{\boldsymbol{v}_t}+\epsilon}$, the update rule becomes $\boldsymbol{x}_{t+1} = \boldsymbol{x}_t - \gamma \frac{\boldsymbol{m}_t}{\sqrt{\boldsymbol{v}_t}+\epsilon} = \boldsymbol{x}_t - \gamma \frac{|\boldsymbol{m}_t|}{\sqrt{\boldsymbol{v}_t}+\epsilon} \circ \frac{\boldsymbol{m}_t}{|\boldsymbol{m}_t|} = \boldsymbol{x}_t - \gamma \boldsymbol{u}_t \circ \mathrm{Sign}(\boldsymbol{m}_t)$. We further have

$$\begin{aligned} \mathbb{E}[F(\boldsymbol{x}_{t+1})] \leq & F(\boldsymbol{x}_t) - \gamma \mathbb{E}[\|\boldsymbol{u}_t \nabla F(\boldsymbol{x}_t)\|_1] + \underbrace{\gamma \mathbb{E}[\langle \nabla F(\boldsymbol{x}_t), \boldsymbol{u}_t \circ (\mathrm{Sign}(\nabla F(\boldsymbol{x}_t)) - \mathrm{Sign}(\boldsymbol{m}_t)) \rangle]}_{\mathcal{T}_1} \\ & + \underbrace{\frac{\gamma^2 (L_0 + L_q \|\nabla F(\boldsymbol{x}_t)\|_2^q)}{2} \mathbb{E}[\|\boldsymbol{u}_t\|_2^2]}_{\mathcal{T}_2}. \end{aligned} \tag{13}$$

Next, we define $R := \frac{1-\beta_1}{\sqrt{(1-\beta_2)(1-\beta_1^2/\beta_2)}}$, and by applying Lemma 2 in the appendix, we obtain that $\boldsymbol{u}_t^{(j)} \leq R$. Furthermore, Lemma 3 in the appendix indicates $\mathbb{E}[|\mathrm{Sign}(\nabla F(\boldsymbol{x}_t^{(j)})) - \mathrm{Sign}(\boldsymbol{m}_t^{(j)})|] \leq 2 \frac{\mathbb{E}[|\nabla F(\boldsymbol{x}_t^{(j)}) - \boldsymbol{m}_t^{(j)}|]}{|\nabla F(\boldsymbol{x}_t^{(j)})|}$, which leads to $\mathcal{T}_1 \leq 2\gamma R \sqrt{d} \mathbb{E}[\|\nabla F(\boldsymbol{x}_t) - \boldsymbol{m}_t\|_2]$.

Employing the bound $\boldsymbol{u}_t^{(j)} \leq R$ above and applying Young's inequality, we obtain $\mathcal{T}_2 \leq \frac{\gamma^2 R^2 d (L_0 + L_1((1-q) + q\mathbb{E}[\|\nabla F(\boldsymbol{x}_t)\|_2]))}{2}$.

By taking the expectation over the first to the $(T-1)$-th iteration, and then summing and rearranging the terms, we obtain:

$$\begin{aligned} & \frac{1}{T} \sum_{t=1}^{T} \mathbb{E}[\|\boldsymbol{u}_t \circ \nabla F(\boldsymbol{x}_t)\|_1] - \frac{\gamma R^2 q L_1 d}{2T} \sum_{t=1}^{T} \mathbb{E}[\|\nabla F(\boldsymbol{x}_t)\|_2] \\ \leq & \frac{F(\boldsymbol{x}_1) - F^*}{\gamma T} + \frac{2R\sqrt{d}}{T} \sum_{t=1}^{T} \mathbb{E}[\|\boldsymbol{m}_t - \nabla F(\boldsymbol{x}_t)\|_2] + \frac{\gamma R^2 d (L_0 + (1-q) L_1)}{2T}. \end{aligned} \tag{14}$$

We now divide-and-conquer prove that

$$\begin{aligned}\frac{1}{T}\sum_{t=1}^{T}\mathbb{E}\left[\|\boldsymbol{m}_t-\nabla F(\boldsymbol{x}_t)\|_2\right] \leq & \frac{\|\nabla F(\boldsymbol{x}_1)\|_2}{T(1-\beta_1)}+\sqrt{1-\beta_1}\left(\sigma_0+\sqrt{\frac{2-p}{2}}\sigma_1\right) \\ & +C_0\sigma_1\sqrt{p(1-\beta_1)}\cdot\frac{1}{T}\sum_{t=1}^{T}\|\nabla F(x_t)\|_2 \\ & +\frac{\gamma R\sqrt{d}(L_0+(1-q)L_1)}{1-\beta_1}+\frac{\gamma R\sqrt{d}qL_1}{1-\beta_1}\cdot\frac{1}{T}\sum_{t=1}^{T}\mathbb{E}[\|\nabla F(\boldsymbol{x}_t)\|_2]\end{aligned} \tag{15}$$

Then, we have

$$\begin{aligned}&\frac{1}{T}\left(\sum_{t=1}^{T}\mathbb{E}[\|\boldsymbol{u}_t\circ\nabla F(\boldsymbol{x}_t)\|_1]-\left(\frac{\gamma R^2dqL_1}{2}+2C_0R\sqrt{d}\sigma_1\sqrt{p(1-\beta_1)}+\frac{2\gamma R^2dqL_1}{1-\beta_1}\right)\sum_{t=1}^{T}\mathbb{E}[\|\nabla F(\boldsymbol{x}_t)\|_2]\right) \\ &\leq\frac{F(\boldsymbol{x}_1)-F^*}{\gamma T}+\frac{2R\sqrt{d}\,\|\nabla F(\boldsymbol{x}_1)\|_2}{T(1-\beta_1)}+2\sqrt{1-\beta_1}R\sqrt{d}\hat{\sigma}+\frac{2\gamma R^2d\hat{L}}{1-\beta_1}+\frac{\gamma R^2d\hat{L}}{2T}.\end{aligned} \tag{16}$$

where $\hat{L}:=L_0+(1-q)L_1$, and $\hat{\sigma}:=\sigma_0+\sqrt{\frac{2-p}{2}}$.

By choosing $\bar{v}=\min_t\mathbb{E}[\boldsymbol{u}_t^{(j)}]$ and applying Condition 2 and Condition 3, we obtain

$$\sum_{t=1}^{T}\mathbb{E}[\|\boldsymbol{u}_t\circ\nabla F(\boldsymbol{x}_t)\|_1]=\sum_{t=1}^{T}\mathbb{E}[\boldsymbol{u}_t^{(j)}]\mathbb{E}[\|\nabla F(\boldsymbol{x}_t)\|_1]\geq\bar{v}\sum_{t=1}^{T}\mathbb{E}[\|(\nabla F(\boldsymbol{x}_t))\|_1]=\frac{\bar{v}\sqrt{d}}{C_1}\sum_{t=1}^{T}\mathbb{E}[\|(\nabla F(\boldsymbol{x}_t))\|_2]. \tag{17}$$

Using generalized Young's inequality, we minimize the bottleneck terms to achieve the lowest bound on the right-hand side of Eq. (16), *i.e.*,

$$\frac{C_1(F(\boldsymbol{x}_1)-F^*)}{\gamma T\sqrt{d}}+2C_1\sqrt{1-\beta_1}R\hat{\sigma}+\frac{2C_1\gamma R^2\sqrt{d}\hat{L}}{1-\beta_1}\geq\frac{512^{1/4}C_1R\hat{\sigma}^{1/2}\hat{L}^{1/4}(F(\boldsymbol{x}_1)-F^*)}{T^{1/4}}, \tag{18}$$

where the lowest bound achieved if and only if $\gamma=\frac{(F(\boldsymbol{x}_1)-F^*)^{3/4}}{2^{1/4}T^{3/4}d^{1/2}R\hat{\sigma}^{1/2}\hat{L}^{1/4}}$ and $1-\beta_1=\frac{2^{1/2}\hat{L}^{1/2}(F(\boldsymbol{x}_1)-F^*)^{1/2}}{T^{1/2}\hat{\sigma}}$.

Now, choosing $\hat{C}_2=\frac{(F(\boldsymbol{x}_1)-F^*)^{3/4}}{2^{1/4}R\hat{\sigma}^{1/2}\hat{L}^{1/4}}$, $\hat{C}_3=\frac{2^{1/2}\hat{L}^{1/2}(F(\boldsymbol{x}_1)-F^*)^{1/2}}{\hat{\sigma}}$, $\gamma=\frac{\hat{C}_2}{T^{3/4}d^{1/2}}$, $1-\beta_1=\frac{\hat{C}_3}{T^{1/2}}$ and setting $T\geq(\frac{4C_0C_1\hat{C}_3{}^{1/2}p^{1/2}R\sigma_1}{\bar{v}}+\frac{4C_1\hat{C}_2R^2qL_1}{\hat{C}_3\bar{v}}+(\frac{C_1\hat{C}_2R^2qL_1}{\bar{v}})^{1/3})^4$, we arrive Case 2 of Corollary 3, *i.e.*,

$$\frac{1}{T}\sum_{t=1}^{T}\mathbb{E}[\|\nabla F(\boldsymbol{x}_t)\|_2]\leq\frac{C_1}{\bar{v}}\left(\frac{512^{1/4}R\hat{\sigma}^{1/2}\hat{L}^{1/4}(F(\boldsymbol{x}_1)-F^*)^{1/4}}{T^{1/4}}+\frac{2C_1R\,\|\nabla F(\boldsymbol{x}_1)\|_2}{\hat{C}_3T^{1/2}}+\frac{\hat{C}_2R^2\hat{L}}{T^{3/4}}\right). \tag{19}$$

5 Conclusion

This work breaks with convention and provides a pioneering reinterpretation of Adam as a sign-like descent algorithm to analyze the convergence, simplifying its theoretical analysis and addressing limitations of the traditional preconditioned perspective. By treating $\frac{|\boldsymbol{m}_t|}{\sqrt{\boldsymbol{v}_t}+\epsilon}$ as a unified random variable, this is the first time that it have been proved that Adam dimension-freely and ϵ-freely achieves the optimal convergence rate of $\mathcal{O}(\frac{1}{T^{1/4}})$ under the weak assumptions of generalized (L_0,L_1,q)-smoothness and affine variance.

REFERENCES

Yossi Arjevani, Yair Carmon, John C Duchi, Dylan J Foster, Nathan Srebro, and Blake Woodworth. Lower bounds for non-convex stochastic optimization. *Mathematical Programming*, 199(1-2):165–214, 2023.

Amit Attia and Tomer Koren. SGD with AdaGrad stepsizes: Full adaptivity with high probability to unknown parameters, unbounded gradients and affine variance. In *International Conference on Machine Learning*, pp. 1147–1171. PMLR, 2023.

Lukas Balles and Philipp Hennig. Dissecting Adam: The sign, magnitude and variance of stochastic gradients. In *International Conference on Machine Learning*, pp. 404–413, 2018.

Jeremy Bernstein, Yu-Xiang Wang, Kamyar Azizzadenesheli, and Animashree Anandkumar. signSGD: Compressed optimisation for non-convex problems. In *International Conference on Machine Learning*, pp. 560–569, 2018.

Dimitri P Bertsekas and John N Tsitsiklis. Gradient convergence in gradient methods with errors. *SIAM Journal on Optimization*, 10(3):627–642, 2000.

Léon Bottou, Frank E Curtis, and Jorge Nocedal. Optimization methods for large-scale machine learning. *SIAM review*, 60(2):223–311, 2018.

Tom Brown, Benjamin Mann, Nick Ryder, Melanie Subbiah, Jared D Kaplan, Prafulla Dhariwal, Arvind Neelakantan, Pranav Shyam, Girish Sastry, Amanda Askell, et al. Language models are few-shot learners. *Advances in neural information processing systems*, 33:1877–1901, 2020.

Congliang Chen, Li Shen, Fangyu Zou, and Wei Liu. Towards practical Adam: Non-convexity, convergence theory, and mini-batch acceleration. *Journal of Machine Learning Research*, 23(229):1–47, 2022.

Lizhang Chen, Bo Liu, Kaizhao Liang, and Qiang Liu. Lion secretly solves constrained optimization: As lyapunov predicts. *arXiv preprint arXiv:2310.05898*, 2023a.

Xiangning Chen, Chen Liang, Da Huang, Esteban Real, Kaiyuan Wang, Yao Liu, Hieu Pham, Xuanyi Dong, Thang Luong, Cho-Jui Hsieh, et al. Symbolic discovery of optimization algorithms. *arXiv preprint arXiv:2302.06675*, 2023b.

Xiangyi Chen, Sijia Liu, Ruoyu Sun, and Mingyi Hong. On the convergence of a class of Adam-type algorithms for non-convex optimization. *arXiv preprint arXiv:1808.02941*, 2018.

Aakanksha Chowdhery, Sharan Narang, Jacob Devlin, Maarten Bosma, Gaurav Mishra, Adam Roberts, Paul Barham, Hyung Won Chung, Charles Sutton, Sebastian Gehrmann, et al. PaLM: Scaling language modeling with pathways. *Journal of Machine Learning Research*, 24(240):1–113, 2023.

Michael Crawshaw, Mingrui Liu, Francesco Orabona, Wei Zhang, and Zhenxun Zhuang. Robustness to unbounded smoothness of generalized signSGD. In *Advances in neural information processing systems*, pp. 9955–9968, 2022.

Alexandre Défossez, Léon Bottou, Francis Bach, and Nicolas Usunier. A simple convergence proof of Adam and AdaGrad. *arXiv preprint arXiv:2003.02395*, 2020.

Abhimanyu Dubey, Abhinav Jauhri, Abhinav Pandey, Abhishek Kadian, Ahmad Al-Dahle, Aiesha Letman, Akhil Mathur, Alan Schelten, Amy Yang, Angela Fan, et al. The Llama 3 herd of models. *arXiv preprint arXiv:2407.21783*, 2024.

Matthew Faw, Isidoros Tziotis, Constantine Caramanis, Aryan Mokhtari, Sanjay Shakkottai, and Rachel Ward. The power of adaptivity in SGD: Self-tuning step sizes with unbounded gradients and affine variance. In *Conference on Learning Theory*, pp. 313–355. PMLR, 2022.

Matthew Faw, Litu Rout, Constantine Caramanis, and Sanjay Shakkottai. Beyond uniform smoothness: A stopped analysis of adaptive SGD. In *The Thirty Sixth Annual Conference on Learning Theory*, pp. 89–160. PMLR, 2023.

Kaiming He, Xiangyu Zhang, Shaoqing Ren, and Jian Sun. Deep residual learning for image recognition. In *IEEE Conference on Computer Vision and Pattern Recognition*, pp. 770–778, 2016.

Geoffrey Hinton, Nitish Srivastava, and Kevin Swersky. Neural networks for machine learning lecture 6a overview of mini-batch gradient descent. *Cited on*, 14(8):2, 2012.

Yusu Hong and Junhong Lin. High probability convergence of Adam under unbounded gradients and affine variance noise. *arXiv preprint arXiv:2311.02000*, 2023.

Yusu Hong and Junhong Lin. On convergence of Adam for stochastic optimization under relaxed assumptions. *Advances in Neural Information Processing Systems*, 2025.

Florian Hübler, Junchi Yang, Xiang Li, and Niao He. Parameter-agnostic optimization under relaxed smoothness. In *International Conference on Artificial Intelligence and Statistics*, pp. 4861–4869. PMLR, 2024.

Jikai Jin, Bohang Zhang, Haiyang Wang, and Liwei Wang. Non-convex distributionally robust optimization: Non-asymptotic analysis. In *Advances in Neural Information Processing Systems*, volume 34, pp. 2771–2782, 2021.

Keller Jordan, Yuchen Jin, Vlado Boza, Jiacheng You, Franz Cesista, Laker Newhouse, and Jeremy Bernstein. Muon: An optimizer for hidden layers in neural networks. *https://kellerjordan.github.io/posts/muon/*, 2024.

Hamed Karimi, Julie Nutini, and Mark Schmidt. Linear convergence of gradient and proximal-gradient methods under the polyak-łojasiewicz condition. In *Machine Learning and Knowledge Discovery in Databases: European Conference, ECML-PKDD-2016*, pp. 795–811, 2016.

Diederik Kingma and Jimmy Ba. Adam: A method for stochastic optimization. In *International Conference on Learning Representations (ICLR)*, 2015.

Alexander Kirillov, Eric Mintun, Nikhila Ravi, Hanzi Mao, Chloe Rolland, Laura Gustafson, Tete Xiao, Spencer Whitehead, Alexander C Berg, Wan-Yen Lo, et al. Segment anything. *arXiv preprint arXiv:2304.02643*, 2023.

Alex Krizhevsky, Ilya Sutskever, and Geoffrey E Hinton. Imagenet classification with deep convolutional neural networks. *Communications of the ACM*, 60(6):84–90, 2017.

Frederik Kunstner, Jacques Chen, Jonathan Wilder Lavington, and Mark Schmidt. Noise is not the main factor behind the gap between SGD and Adam on transformers, but sign descent might be. *arXiv preprint arXiv:2304.13960*, 2023.

Frederik Kunstner, Robin Yadav, Alan Milligan, Mark Schmidt, and Alberto Bietti. Heavy-tailed class imbalance and why Adam outperforms gradient descent on language models. *arXiv preprint arXiv:2402.19449*, 2024.

Haochuan Li, Alexander Rakhlin, and Ali Jadbabaie. Convergence of Adam under relaxed assumptions. *Advances in Neural Information Processing Systems*, 36, 2023.

Jingyuan Liu, Jianlin Su, Xingcheng Yao, Zhejun Jiang, Guokun Lai, Yulun Du, Yidao Qin, Weixin Xu, Enzhe Lu, Junjie Yan, et al. Muon is scalable for llm training. *arXiv preprint arXiv:2502.16982*, 2025.

Yanli Liu, Yuan Gao, and Wotao Yin. An improved analysis of stochastic gradient descent with momentum. *Advances in Neural Information Processing Systems*, 33:18261–18271, 2020.

Zhuang Liu, Hanzi Mao, Chao-Yuan Wu, Christoph Feichtenhofer, Trevor Darrell, and Saining Xie. A convnet for the 2020s. In *Proceedings of the IEEE/CVF conference on computer vision and pattern recognition*, pp. 11976–11986, 2022.

Alec Radford, Jong Wook Kim, Chris Hallacy, Aditya Ramesh, Gabriel Goh, Sandhini Agarwal, Girish Sastry, Amanda Askell, Pamela Mishkin, Jack Clark, et al. Learning transferable visual models from natural language supervision. In *International conference on machine learning*, pp. 8748–8763, 2021.

Sashank J Reddi, Satyen Kale, and Sanjiv Kumar. On the convergence of Adam and beyond. In *International Conference on Learning Representations*, 2018.

Martin Riedmiller and Heinrich Braun. A direct adaptive method for faster backpropagation learning: The rprop algorithm. In *IEEE international conference on neural networks*, pp. 586–591. IEEE, 1993.

Frank Seide, Hao Fu, Jasha Droppo, Gang Li, and Dong Yu. 1-bit stochastic gradient descent and its application to data-parallel distributed training of speech DNNs. In *Conference of the International Speech Communication Association*, volume 2014, pp. 1058–1062. Singapore, 2014.

Ishaan Shah, Anthony M Polloreno, Karl Stratos, Philip Monk, Adarsh Chaluvaraju, Andrew Hojel, Andrew Ma, Anil Thomas, Ashish Tanwer, Darsh J Shah, et al. Practical efficiency of muon for pretraining. *arXiv preprint arXiv:2505.02222*, 2025.

Naichen Shi, Dawei Li, Mingyi Hong, and Ruoyu Sun. RMSProp converges with proper hyperparameter. In *International Conference on Learning Representation*, 2021.

Nikko Ström. Scalable distributed DNN training using commodity GPU cloud computing. In *Conference of the International Speech Communication Association*, 2015.

Tao Sun, Qingsong Wang, Dongsheng Li, and Bao Wang. Momentum ensures convergence of signSGD under weaker assumptions. In *International Conference on Machine Learning*, pp. 33077–33099, 2023.

Hugo Touvron, Thibaut Lavril, Gautier Izacard, Xavier Martinet, Marie-Anne Lachaux, Timothée Lacroix, Baptiste Rozière, Naman Goyal, Eric Hambro, Faisal Azhar, et al. Llama: Open and efficient foundation language models. *arXiv preprint arXiv:2302.13971*, 2023a.

Hugo Touvron, Louis Martin, Kevin Stone, Peter Albert, Amjad Almahairi, Yasmine Babaei, Nikolay Bashlykov, Soumya Batra, Prajjwal Bhargava, Shruti Bhosale, et al. Llama 2: Open foundation and fine-tuned chat models. *arXiv preprint arXiv:2307.09288*, 2023b.

Ashish Vaswani, Noam Shazeer, Niki Parmar, Jakob Uszkoreit, Llion Jones, Aidan N Gomez, Łukasz Kaiser, and Illia Polosukhin. Attention is all you need. *Advances in neural information processing systems*, 30, 2017.

Bohan Wang, Huishuai Zhang, Zhiming Ma, and Wei Chen. Convergence of AdaGrad for non-convex objectives: Simple proofs and relaxed assumptions. In *Conference on Learning Theory*, pp. 161–190. PMLR, 2023a.

Bohan Wang, Huishuai Zhang, Zhiming Ma, and Wei Chen. Convergence of AdaGrad for non-convex objectives: Simple proofs and relaxed assumptions. In *The Thirty Sixth Annual Conference on Learning Theory*, pp. 161–190. PMLR, 2023b.

Bohan Wang, Yushun Zhang, Huishuai Zhang, Qi Meng, Ruoyu Sun, Zhi-Ming Ma, Tie-Yan Liu, Zhi-Quan Luo, and Wei Chen. Provable adaptivity of Adam under non-uniform smoothness. In *Proceedings of the 30th ACM SIGKDD Conference on Knowledge Discovery and Data Mining*, pp. 2960–2969, 2023c.

Bohan Wang, Huishuai Zhang, Qi Meng, Ruoyu Sun, Zhi-Ming Ma, and Wei Chen. On the convergence of Adam under non-uniform smoothness: Separability from sgdm and beyond. *arXiv preprint arXiv:2403.15146*, 2024.

Sanghyun Woo, Shoubhik Debnath, Ronghang Hu, Xinlei Chen, Zhuang Liu, In So Kweon, and Saining Xie. Convnext v2: Co-designing and scaling convnets with masked autoencoders. In *Proceedings of the IEEE/CVF Conference on Computer Vision and Pattern Recognition*, pp. 16133–16142, 2023.

Greg Yang, Edward J Hu, Igor Babuschkin, Szymon Sidor, Xiaodong Liu, David Farhi, Nick Ryder, Jakub Pachocki, Weizhu Chen, and Jianfeng Gao. Tensor programs V: Tuning large neural networks via zero-shot hyperparameter transfer. *arXiv preprint arXiv:2203.03466*, 2022.

Bohang Zhang, Jikai Jin, Cong Fang, and Liwei Wang. Improved analysis of clipping algorithms for non-convex optimization. In *Advances in Neural Information Processing Systems*, volume 33, pp. 15511–15521, 2020.

Jingzhao Zhang, Tianxing He, Suvrit Sra, and Ali Jadbabaie. Why gradient clipping accelerates training: A theoretical justification for adaptivity. In *International Conference on Learning Representations*, 2019.

Yushun Zhang, Congliang Chen, Naichen Shi, Ruoyu Sun, and Zhi-Quan Luo. Adam can converge without any modification on update rules. *Advances in neural information processing systems*, 35:28386–28399, 2022.

Appendix

The Use of Large Language Models (LLMs). The use of LLMs in the preparation of this work is confined to that of a polishing and assistive tool. They were not involved in the core intellectual processes of research ideation, hypothesis formation, or theoretical derivation. Their role was limited to tasks such as checking grammar, refining sentence structure, and improving the clarity of text that was entirely conceived and drafted by the human authors.

A Relate Work

There is a large amount of works on the theoretical analysis of stochastic descents algorithms. In this section, we list the most related references and make comparison with our work.

Convergence with Weak Assumptions. Bertsekas & Tsitsiklis (2000) first theoretically analyze SGD under the assumption of affine variances, obtaining an asymptotic convergence result. Until 2018, Bottou et al. (2018) proved the non-asymptotic convergence rate of $\|\nabla F(x)\|_2$ for SGD up to $\mathcal{O}\left(\frac{\text{poly}(\ln T)}{T^{1/4}}\right)$, which matched its provable rate with the bounded variance condition. In terms of adaptive optimizers, Faw et al. (2022) investigated the convergence rate of AdaGrad-Norm with the affine variance, and proved the rate could achieve $\mathcal{O}\left(\frac{\text{poly}(\ln T)}{T^{1/4}}\right)$ as well when $\sigma_1 = \mathcal{O}\left(\frac{1}{\sqrt{T}}\right)$. Wang et al. (2023a) proved the AdaGrad-Norm obtained a similar convergence rate with no restriction over σ_1, and it further demonstrate vanilla AdaGrad could also achieve the same convergence rate under a stronger assumption of coordinate-wise affine variances. Meanwhile, Attia & Koren (2023) provided a probabilistic convergence rate for AdaGrad-Norm. Noted that Shi et al. (2021) and Zhang et al. (2022) respectively proved random-shuffled AMSProp and Adam will converge to the neighbourhood of stationary points with the rate $\mathcal{O}\left(\frac{\text{poly}(\ln E)}{E^{1/4}} + \sigma_0\right)$ where E is the number of epoches rather than iterations under the affine growth condition that is equivalent to the affine variance condition, which is much slower than the optimal rate. Recently, Hong & Lin (2023) provably demonstrate the convergence rate of vanilla Adam in high probability perspective, but it only works with the stronger coordinate-wise affine variance.

Zhang et al. (2019) first introduced the unciform (L_0, L_1)-smooth condition to theoretically explain why Clipped-SGD converges faster than vanilla SGD, and they also empirically verified that local smoothness indeed varies with the norm of gradients during DNN training. Zhang et al. (2020) posits that it is also equivalent to an affine form of the gradient norm for the first-order differentiable function. Then, this relaxed assumption is extended to analyzing clipping-SGD with momentum Zhang et al. (2020), distributionally robust optimization Jin et al. (2021), normalized SGD with momentum Hübler et al. (2024), generalized signSGD Crawshaw et al. (2022). Recently, Wang et al. (2023c) theoretically analyzing random-shuffled Adam under this condition, but its convergence rate is provable $\mathcal{O}\left(\frac{\text{poly}(\ln E)}{E^{1/4}}\right)$ where E is the number of epoch, just like Zhang et al. (2022). Li et al. (2023) further extended the linear (L_0, L_1)-smooth to the generalized polynomial version, and proved that Adam will converged to $\mathcal{O}\left(\frac{\text{poly}(\ln T)}{T^{1/4}}\right)$ with the weaker assumption. However, the bound heavily relies on a large ϵ , but Adam with a large ϵ is essentially similar to SGD and loses the nature of adaptivity.

Furthermore, Faw et al. (2023); Wang et al. (2023b) theoretically analyze AdaGrad under the weak assumptions of both affine variance and non-uniform (L_0, L_1)-smoothness, also obtaining the rate of $\mathcal{O}\left(\frac{\text{poly}(\ln T)}{T^{1/4}}\right)$. Wang et al. (2024) also provable provide a high probability convergence of a simplified Adam-Norm with the both weak assumptions. More recently, Hong & Lin (2025) prove the convergence rate of vanilla Adam with both the affine variance condition and the (L_0, L_1)-smooth condition, but its proof have a fatal error that may vacuum the validity (The constant and T-independent G is the premise of the theoretical analysis,

but $1-\beta_2=\mathcal{O}(\frac{1}{T})$, $1-\beta_2=\frac{c}{T}$, Eq. (41), Eq. (56) and Eq. (58) in the proof suggest that $\|\bar{\boldsymbol{g}}_{t+1}\|^2$ should be larger than $\mathcal{O}(T)$.).

In comparison to the convergence analyses above, we are the first to formally analyze vanilla under the weak assumptions of the generalized affine variance and the generalized unciform (L_0, L_1)-smooth, achieving a tighter bound of $\mathcal{O}\left(\frac{1}{T^{1/4}}\right)$ rather than$\mathcal{O}\left(\frac{\text{poly}(\ln T)}{T^{1/4}}\right)$.

Convergence of Sign Descent. Sign-based algorithms that simply exploits the signs of gradients could date back to RPROP (Riedmiller & Braun (1993)). Seide et al. (2014); Ström (2015) proposed 1-bit SGD and empirically demonstrate it achieve good performance while dramatically reducing the communication costs in distributed system. The non-stochastic convergence proof of signSGD was first analyzed in (Karimi et al. (2016)) under the Polyak-Łojasiewicz condition. Then, Bernstein et al. (2018) systematically establish the convergence rate of signSGD in stochastic and non-convex scenario, but it required an increasing batch size up to $O(\sqrt{n})$ where n is the number of samples to guarantee convergence. Then, Sun et al. (2023) first proved that momentum can ensures the convergence of signSGD without increasing batch size. Chen et al. (2023b) employs an AutoML method to discover an effective optimizer, Lion, resembling signSGD with momentum, and demonstrate superior performance to Adam across diverse DNN models. Chen et al. (2023a) theoretically analyzed the efficacy of Lion but did not provide the convergence proof. Meanwhile, the original version of Adam, RMSProp Hinton et al. (2012), were developed from the sign-based Rprop. Balles & Hennig (2018) also found that sign descent algorithms has a deep connection with Adam. Recently, Kunstner et al. (2023; 2024) empirically showcase that the sign-like property of Adam is just the primary reason behind its superior performance for training DNNs. In short, signSGD has a close connection with Adam, but the existing convergence proofs of Adam were not built upon this connection. More recently, Muon Jordan et al. (2024), an extended matrix-sign optimizer, has demonstrated significant potential for training DNNs Liu et al. (2025); Shah et al. (2025), although its current implementation is confined to parameters with a 2D structure.

To the best of our knowledge, our work is the first to prove the convergence rate of Adam from the perspective of sign descent, and the proof, thereby, becomes considerably simple, compared to the previous theoretical proofs of Adam.

B Theoretical Analysis

B.1 Proof of Proposition 2.1

Proof. It is known that

$$\begin{aligned}\frac{1}{T}\sum_{t=1}^{T}\|\nabla F(\boldsymbol{x}_t)\|_2^2 =&\Theta\left(\frac{1}{T}\sum_{t=1}^{T}\frac{1}{t^{2\alpha}}\right)\\ \leq&\mathcal{O}\left(\frac{1}{T}\int_{t=1}^{T}\frac{1}{t^{2\alpha}}dt\right)\\ =&\mathcal{O}\left(\frac{T^{1-2\alpha}-1}{T(1-2\alpha)}\right)\\ \leq&\mathcal{O}\left(\frac{1}{1-2\alpha}\cdot\frac{1}{T^{2\alpha}}\right).\end{aligned} \tag{20}$$

and

$$\begin{aligned}\left(\frac{1}{T}\sum_{t=1}^{T}\|\nabla F(\boldsymbol{x}_t)\|_2\right)^2 =&\Theta\left(\left(\frac{1}{T}\sum_{t=1}^{T}\frac{1}{t^\alpha}\right)^2\right)\\ \geq&\Omega\left(\left(\frac{1}{T}\int_{t=2}^{T+1}\frac{1}{t^\alpha}dt\right)^2\right)\\ \geq&\Omega\left(\frac{1}{(1-\alpha)^2}\cdot\left(\frac{1}{T^{2\alpha}}-\frac{2^{1-\alpha}}{T^{1+\alpha}}\right)\right).\end{aligned} \tag{21}$$

It is easy to verify that when $T \geq 2^{\frac{2-\alpha}{1-\alpha}}$, $\frac{2^{1-\alpha}}{T^{1+\alpha}} \leq \frac{1}{2}\cdot\frac{1}{T^{2\alpha}}$. Moreover, we can obtain $2^{\frac{2-\alpha}{1-\alpha}} \leq 8$ due to $0 \leq \alpha < \frac{1}{2}$. Hence, when $T \geq 8$, we have

$$\frac{\frac{1}{T}\sum_{t=1}^{T}\|\nabla F(\boldsymbol{x}_t)\|_2^2}{\left(\frac{1}{T}\sum_{t=1}^{T}\|\nabla F(\boldsymbol{x}_t)\|_2\right)^2} \leq \mathcal{O}\left(\frac{2(1-\alpha)^2}{1-2\alpha}\right). \tag{22}$$

B.2 Useful Lemmas

Lemma 1 *Under Assumption B.3, for any $\boldsymbol{x}, \boldsymbol{y} \in \mathbb{R}^d$, the function obeys*

$$F(\boldsymbol{y}) \leq F(\boldsymbol{x}) + \langle\nabla F(\boldsymbol{x}), \boldsymbol{y}-\boldsymbol{x}\rangle + \frac{L_0 + L_1\|\nabla F(\boldsymbol{x})\|_2^q}{2}\|\boldsymbol{y}-\boldsymbol{x}\|_2^2. \tag{23}$$

Proof. For any $\boldsymbol{x}, \boldsymbol{y} \in \mathbb{R}^d$, we have

$$\begin{aligned}F(\boldsymbol{y}) =&F(\boldsymbol{x}) + \int_0^1\langle\nabla F(\boldsymbol{x}+t(\boldsymbol{y}-\boldsymbol{x})), \boldsymbol{y}-\boldsymbol{x}\rangle dt\\ =&F(\boldsymbol{x}) + \langle\nabla F(\boldsymbol{x}), \boldsymbol{y}-\boldsymbol{x}\rangle + \int_0^1\langle\nabla F(\boldsymbol{x}+t(\boldsymbol{y}-\boldsymbol{x})) - \nabla F(\boldsymbol{x}), \boldsymbol{y}-\boldsymbol{x}\rangle dt\\ \overset{(i)}{\leq}&F(\boldsymbol{x}) + \langle\nabla F(\boldsymbol{x}), \boldsymbol{y}-\boldsymbol{x}\rangle + \int_0^1\|\nabla F(\boldsymbol{x}+t(\boldsymbol{y}-\boldsymbol{x})) - \nabla F(\boldsymbol{x})\|_2\|\boldsymbol{y}-\boldsymbol{x}\|_2 dt\\ \overset{(ii)}{\leq}&F(\boldsymbol{x}) + \langle\nabla F(\boldsymbol{x}), \boldsymbol{y}-\boldsymbol{x}\rangle + (L_0 + L_1\|\nabla F(\boldsymbol{x})\|_2^q)\|\boldsymbol{y}-\boldsymbol{x}\|_2^2\int_0^1 t d_t\\ =&F(\boldsymbol{x}) + \langle\nabla F(\boldsymbol{x}), \boldsymbol{y}-\boldsymbol{x}\rangle + \frac{L_0 + L_1\|\nabla F(\boldsymbol{x})\|_2^q}{2}\|\boldsymbol{y}-\boldsymbol{x}\|_2^2,\end{aligned} \tag{24}$$

where(i) holds due to Cauchy-Schwarz inequality, and (ii) holds due to Assumption 2.

Lemma 2 *Let the sequences $\{\hat{\boldsymbol{m}}_t\}$ and $\{\hat{\boldsymbol{v}}_t\}$ be generated by Adam in Algorithm 1. If the moving average coefficients β_1, β_2 are constant and satisfy $\beta_1^2 < \beta_2$, then*

(1) For any $j \in [d]$, it holds that

$$\frac{|\hat{\boldsymbol{m}}_t^{(j)}|}{\sqrt{\hat{\boldsymbol{v}}_t^{(j)}} + \epsilon} \leq \frac{1-\beta_1}{\sqrt{1-\beta_2}\sqrt{1-\frac{\beta_1^2}{\beta_2}}}. \tag{25}$$

(2) The maximal value of $\frac{1-\beta_1}{\sqrt{1-\beta_2}\sqrt{1-\frac{\beta_1^2}{\beta_2}}}$ *is lower bounded by* 1*, and upper bounded by* $\sqrt{\frac{1-\beta_1}{1-\beta_2}}$ *when* $\beta_1 \leq \beta_2$.

Proof. (1) Recalling Adam, we know

$$\begin{aligned}\hat{\boldsymbol{m}}_t^{(j)} &= \frac{1-\beta_1}{1-\beta_1^t}\sum_{k=1}^{t}\beta_1^{t-k}\boldsymbol{g}_k^{(j)} \\ \hat{\boldsymbol{v}}_t^{(j)} &= \frac{1-\beta_2}{1-\beta_2^t}\sum_{k=1}^{t}\beta_2^{t-k}(\boldsymbol{g}_k^{(j)})^2.\end{aligned} \tag{26}$$

Then,

$$\begin{aligned}\frac{|\boldsymbol{m}_t^{(j)}|}{\sqrt{\boldsymbol{v}_t^{(j)}}+\epsilon} \leq& \frac{(1-\beta_1)\sqrt{1-\beta_2^t}}{(1-\beta_1^t)\sqrt{1-\beta_2}}\cdot\frac{|\sum_{k=1}^{t}\beta_1^{t-k}\boldsymbol{g}_k^{(j)}|}{\sqrt{\sum_{k=1}^{t}\beta_2^{t-k}(\boldsymbol{g}_k^{(j)})^2}} \\ \overset{(i)}{\leq}& \frac{(1-\beta_1)\sqrt{1-\beta_2^t}}{(1-\beta_1^t)\sqrt{1-\beta_2}}\cdot\frac{\sum_{k=1}^{t}\beta_1^{t-k}|\boldsymbol{g}_k^{(j)}|}{\sqrt{\sum_{k=1}^{t}\beta_2^{t-k}(\boldsymbol{g}_k^{(j)})^2}} \\ \overset{(ii)}{\leq}& \frac{(1-\beta_1)\sqrt{1-\beta_2^t}}{(1-\beta_1^t)\sqrt{1-\beta_2}}\cdot\frac{\sqrt{\sum_{k=1}^{t}\beta_2^{t-k}(\boldsymbol{g}_k^{(j)})^2}\sqrt{\sum_{k=1}^{t}\frac{\beta_1^{2(t-k)}}{\beta_2^{t-k}}}}{\sqrt{\sum_{k=1}^{t}\beta_2^{t-k}(\boldsymbol{g}_k^{(j)})^2}} \\ =& \frac{(1-\beta_1)\sqrt{1-\beta_2^t}}{(1-\beta_1^t)\sqrt{1-\beta_2}}\cdot\sqrt{\sum_{k=1}^{t}\left(\frac{\beta_1^2}{\beta_2}\right)^{t-k}} \\ \overset{(iii)}{=}& \frac{(1-\beta_1)\sqrt{1-\beta_2^t}}{(1-\beta_1^t)\sqrt{1-\beta_2}}\cdot\frac{\sqrt{1-\left(\frac{\beta_1^2}{\beta_2}\right)^t}}{\sqrt{1-\frac{\beta_1^2}{\beta_2}}} \\ \overset{(iv)}{\leq}& \frac{1-\beta_1}{\sqrt{1-\beta_2}\sqrt{1-\frac{\beta_1^2}{\beta_2}}},\end{aligned} \tag{27}$$

where (i) holds due to the fact $|\boldsymbol{a}^{(j)}+\boldsymbol{b}^{(j)}| \leq |\boldsymbol{a}^{(j)}|+|\boldsymbol{b}^{(j)}|$; (ii) holds resulting from Cauchy-Schwarz inequality; (iii) holds since $\beta_1^2 \leq \beta_2$; (iv) holds owing to the fact that $1-\frac{a^2}{b} \leq \frac{(1-a)^2}{1-b}$.

(2) The maximal value of $\frac{|\boldsymbol{m}_t^{(j)}|}{\sqrt{\boldsymbol{v}_t^{(j)}}}$ is lower bounded by

$$\frac{1-\beta_1}{\sqrt{1-\beta_2}\sqrt{1-\frac{\beta_1^2}{\beta_2}}} \geq \frac{1-\beta_1}{1-\frac{1}{2}(\beta_2+\frac{\beta_1^2}{\beta_2})} \geq \frac{1-\beta_1}{1-\beta_1} = 1, \tag{28}$$

where the first and second inequality reaches the lower bound if and only $\beta_1 = \beta_2$.

When $\beta_1 \leq \beta_2$, the maximal value of $\frac{|\boldsymbol{m}_t^{(j)}|}{\sqrt{\boldsymbol{v}_t^{(j)}}}$ is upper bounded by

$$\frac{1-\beta_1}{\sqrt{1-\beta_2}\sqrt{1-\frac{\beta_1^2}{\beta_2}}} \leq \frac{1-\beta_1}{\sqrt{1-\beta_2}\sqrt{1-\frac{\beta_1\beta_2}{\beta_2}}} = \frac{\sqrt{1-\beta_1}}{\sqrt{1-\beta_2}}. \tag{29}$$

Lemma 3 *For any random variable $\mathcal{Z}$ and a constant C, there exists*

$$\mathbb{E}[|\text{Sign}(\mathcal{Z}) - \text{Sign}(C)|] \leq \frac{2\mathbb{E}[|\mathcal{Z} - C|]}{|C|}. \tag{30}$$

Proof. Using Markov'equality, we direct obtain

$$\begin{aligned}\mathbb{E}[|\text{Sign}(\mathcal{Z}) - \text{Sign}(C)|] =& 2\mathbb{P}[\mathbb{I}(\text{Sign}(\mathcal{Z}) \neq \text{Sign}(C))] \\ \leq& 2\mathbb{P}[|\mathcal{Z} - C| \geq |C|] \\ \leq& \frac{2\mathbb{E}[|\mathcal{Z} - C|]}{|C|}.\end{aligned} \tag{31}$$

Lemma 4 *Let $a, b > 0$ and $0 < \alpha < \beta$. If $x \geq (a + b^{\alpha/\beta})^{1/\alpha}$, then $\frac{a}{x^\alpha} + \frac{b}{x^\beta} \leq 1$. The bound is tight up to the factor of 2 since $\frac{(a+b^{\alpha/\beta})^{1/\alpha}}{2} \leq \max(a, b^{\alpha/\beta}) \leq (a + b^{\alpha/\beta})^{1/\alpha}$.*

Proof. Let $s = x^\alpha$ and $\gamma = \frac{\beta}{\alpha} \geq 1$, then the inequality becomes

$$\frac{a}{s} + \frac{b}{s^\gamma} \leq 1 \tag{32}$$

If s^* is a solution of Eq. (32), it should satisfy

$$s^* \geq \max(a, b^{1/\gamma}). \tag{33}$$

When we set $s_+ = a + b^{1/\gamma}$, it is easy to verify that

$$\frac{a}{s_+} + \frac{b}{s_+^\gamma} = \frac{a}{a + b^{1/\gamma}} + \frac{b}{(a + b^{1/\gamma})^\gamma} \leq \frac{a}{a + b^{1/\gamma}} + \frac{b^{1/\gamma}}{a + b^{1/\gamma}} = 1. \tag{34}$$

On the other hand, it is also easy to verify that $s_- = \frac{a+b^{1/\gamma}}{2}$ does not satisfy Eq. (33), which means that s_+ is at most a factor of 2 worse than the smallest solution of Eq. (32), so $x_+ = (a + b^{\alpha/\beta})^{1/\alpha}$ is at most a factor of 2 worse than the smallest solution of $\frac{a}{x^\alpha} + \frac{b}{x^\beta} \leq 1$.

B.3 Proof of Theorem 2

Proof. Following Lemma 1 with $\boldsymbol{x}_{t+1} \to \boldsymbol{y}$ and $\boldsymbol{x}_t \to \boldsymbol{x}$, we have

$$F(\boldsymbol{x}_{t+1}) \leq F(\boldsymbol{x}_t) + \langle \nabla F(\boldsymbol{x}_t), \boldsymbol{x}_{t+1} - \boldsymbol{x}_t \rangle + \frac{L_0 + L_1 \|\nabla F(\boldsymbol{x}_t)\|_2^q}{2} \|\boldsymbol{x}_{t+1} - \boldsymbol{x}_t\|_2^2. \tag{35}$$

Recalling the update rule $\boldsymbol{x}_{t+1} = \boldsymbol{x}_t - \gamma \frac{\hat{\boldsymbol{m}}_t}{\sqrt{\hat{\boldsymbol{v}}_t} + \epsilon} = \boldsymbol{x}_t - \gamma \frac{|\hat{\boldsymbol{m}}_t|}{\sqrt{\hat{\boldsymbol{v}}_t} + \epsilon} \circ \frac{\hat{\boldsymbol{m}}_t}{|\hat{\boldsymbol{m}}_t|} = \boldsymbol{x}_t - \gamma \boldsymbol{u}_t \circ \text{Sign}(\hat{\boldsymbol{m}}_t) = \boldsymbol{x}_t - \gamma \boldsymbol{u}_t \circ \text{Sign}(\boldsymbol{m}_t)$, we further obtain

$$\begin{aligned}F(\boldsymbol{x}_{t+1}) \leq& F(\boldsymbol{x}_t) - \langle \nabla F(\boldsymbol{x}_t), \gamma \boldsymbol{u}_t \circ \text{Sign}(\boldsymbol{m}_t) \rangle + \frac{(L_0 + L_1 \|\nabla F(\boldsymbol{x}_t)\|_2^q)\gamma^2}{2} \|\boldsymbol{u}_t\|_2^2 \\ =& F(\boldsymbol{x}_t) - \langle \nabla F(\boldsymbol{x}_t), \gamma \boldsymbol{u}_t \circ \text{Sign}(\nabla F(\boldsymbol{x}_t)) \rangle + \langle \nabla F(\boldsymbol{x}_t), \gamma \boldsymbol{u}_t \circ (\text{Sign}(\nabla F(\boldsymbol{x}_t)) - \text{Sign}(\boldsymbol{m}_t)) \rangle \\ &+ \frac{\gamma^2 (L_0 + L_1 \|\nabla F(\boldsymbol{x}_t)\|_2^q)}{2} \|\boldsymbol{u}_t\|_2^2 \\ \leq& F(\boldsymbol{x}_t) - \langle \nabla F(\boldsymbol{x}_t), \gamma \boldsymbol{u}_t \circ \text{Sign}(\nabla F(\boldsymbol{x}_t)) \rangle + \gamma R \langle |\nabla F(\boldsymbol{x}_t)|, |\text{Sign}(\nabla F(\boldsymbol{x}_t)) - \text{Sign}(\boldsymbol{m}_t)| \rangle \\ &+ \frac{\gamma^2 R^2 d (L_0 + L_1 \|\nabla F(\boldsymbol{x}_t)\|_2^q)}{2},\end{aligned} \tag{36}$$

where the last inequality holds due to $\boldsymbol{u}_t^{(j)} \leq \frac{1-\beta_1}{\sqrt{1-\beta_2}\sqrt{1-\frac{\beta_1^2}{\beta_2}}} = R, \forall j \in [d]$ according to Lemma 2.

Taking the expectation at the t-th iteration, we obtain

$$\begin{aligned}
\mathbb{E}[F(\boldsymbol{x}_{t+1})] \leq & F(\boldsymbol{x}_t) - \gamma\langle \nabla F(\boldsymbol{x}_t), \mathbb{E}[\boldsymbol{u}_t] \circ \mathrm{Sign}(\nabla F(\boldsymbol{x}_t))\rangle + \gamma R\langle |\nabla F(\boldsymbol{x}_t)|, \mathbb{E}[|\mathrm{Sign}(\nabla F(\boldsymbol{x}_t)) - \mathrm{Sign}(\boldsymbol{m}_t)|]\rangle \\
& + \frac{\gamma^2 R^2 d(L_0 + L_1\|\nabla F(\boldsymbol{x}_t)\|_2^q)}{2} \\
\overset{(i)}{\leq} & F(\boldsymbol{x}_t) - \gamma\langle \nabla F(\boldsymbol{x}_t), \mathbb{E}[\boldsymbol{u}_t] \circ \mathrm{Sign}(\nabla F(\boldsymbol{x}_t))\rangle + 2\gamma R\, \mathbb{E}[\|\boldsymbol{m}_t - \nabla F(\boldsymbol{x}_t)\|_1] \\
& + \frac{\gamma^2 R^2 d(L_0 + L_1\|\nabla F(\boldsymbol{x}_t)\|_2^q)}{2} \\
\overset{(ii)}{\leq} & F(\boldsymbol{x}_t) - \gamma\langle \nabla F(\boldsymbol{x}_t), \mathbb{E}[\boldsymbol{u}_t] \circ \mathrm{Sign}(\nabla F(\boldsymbol{x}_t))\rangle + 2\gamma R\sqrt{d}\, \mathbb{E}[\|\boldsymbol{m}_t - \nabla F(\boldsymbol{x}_t)\|_2] \\
& + \frac{\gamma^2 R^2 d(L_0 + L_1\|\nabla F(\boldsymbol{x}_t)\|_2^q)}{2} \\
\overset{(iii)}{\leq} & F(\boldsymbol{x}_t) - \gamma\langle \nabla F(\boldsymbol{x}_t), \mathbb{E}[\boldsymbol{u}_t] \circ \mathrm{Sign}(\nabla F(\boldsymbol{x}_t))\rangle + 2\gamma R\sqrt{d}\, \mathbb{E}[\|\boldsymbol{m}_t - \nabla F(\boldsymbol{x}_t)\|_2] \\
& + \frac{\gamma^2 R^2 d(L_0 + L_1((1-q) + q\|\nabla F(\boldsymbol{x}_t)\|_2))}{2},
\end{aligned} \tag{37}$$

where (i) holds due to $\mathbb{E}[|\mathrm{Sign}(\nabla F(\boldsymbol{x}_t^{(j)})) - \mathrm{Sign}(\boldsymbol{m}_t^{(j)})|] \leq 2\frac{\mathbb{E}[|\nabla F(\boldsymbol{x}_t^{(j)}) - \boldsymbol{m}_t^{(j)}|]}{|\nabla F(\boldsymbol{x}_t^{(j)})|} (\forall j \in [d])$ according to Lemma 3; (ii) holds owing to the fact $\|\boldsymbol{a}\|_1 \leq \sqrt{d}\|\boldsymbol{a}\|_2$ for any $\boldsymbol{a} \in \mathbb{R}^d$; (iii) holds due to the fact $a^q \leq (1-q) + qa$ according to Young's inequality.

Taking expectation from the 1-st iteration to the T-th iteration and then summing them, we have

$$\begin{aligned}
\mathbb{E}[F(\boldsymbol{x}_{t+1})] \leq & F(\boldsymbol{x}_1) - \gamma \sum_{t=1}^{T} \mathbb{E}[\|\boldsymbol{u}_t \circ \nabla F(\boldsymbol{x}_t)\|_1] + 2\gamma R\sqrt{d} \sum_{t=1}^{T} \mathbb{E}[\|\boldsymbol{m}_t - \nabla F(\boldsymbol{x}_t)\|_2] \\
& + \sum_{t=1}^{T} \frac{\gamma^2 R^2 d(L_0 + L_1((1-q) + q\mathbb{E}[\|\nabla F(\boldsymbol{x}_t)\|_2]))}{2}.
\end{aligned} \tag{38}$$

Rearranging the both sides and applying the facts that $F(\boldsymbol{x}_{t+1}) \geq F^*$, we obtain

$$\begin{aligned}
& \frac{1}{T}\sum_{t=1}^{T} \mathbb{E}[\|\boldsymbol{u}_t \circ \nabla F(\boldsymbol{x}_t)\|_1] - \frac{\gamma R^2 q L_1 d}{2T} \sum_{t=1}^{T} \mathbb{E}[\|\nabla F(\boldsymbol{x}_t)\|_2] \\
\leq & \frac{F(\boldsymbol{x}_1) - F^*}{\gamma T} + \frac{2R\sqrt{d}}{T} \sum_{t=1}^{T} \mathbb{E}[\|\boldsymbol{m}_t - \nabla F(\boldsymbol{x}_t)\|_2] + \frac{\gamma R^2 d(L_0 + (1-q)L_1)}{2}.
\end{aligned} \tag{39}$$

Recalling $\boldsymbol{m}_t = \beta_1 \boldsymbol{m}_{t-1} + (1-\beta_1)\boldsymbol{g}_t$, we obtain

$$\begin{aligned}
\boldsymbol{m}_t - \nabla F(\boldsymbol{x}_t) = & (\beta_1 \boldsymbol{m}_{t-1} + (1-\beta_1)\boldsymbol{g}_t) - \nabla F(\boldsymbol{x}_t) \\
= & \beta_1(\boldsymbol{m}_{t-1} - \nabla F(\boldsymbol{x}_{t-1})) + (1-\beta_1)(\boldsymbol{g}_t - \nabla F(\boldsymbol{x}_t)) - \beta_1(\nabla F(\boldsymbol{x}_t) - \nabla F(\boldsymbol{x}_{t-1})).
\end{aligned} \tag{40}$$

Utilizing recursion, we further have

$$\boldsymbol{m}_t - \nabla F(\boldsymbol{x}_t) = -\beta_1^t \nabla F(\boldsymbol{x}_1) + (1-\beta)\sum_{k=1}^{t}\beta_1^{t-k}(\boldsymbol{g}_k - \nabla F(\boldsymbol{x}_k)) - \sum_{k=1}^{t}\beta_1^{t-k+1}(\nabla F(\boldsymbol{x}_k) - \nabla F(\boldsymbol{x}_{k-1})), \tag{41}$$

where $\boldsymbol{m}_1 - \nabla F(\boldsymbol{x}_1) = -\beta_1 \nabla F(\boldsymbol{x}_1) + (1-\beta_1)(\boldsymbol{g}_1 - \nabla F(\boldsymbol{x}_1))$ due to $\boldsymbol{m}_0 = 0$.

Hence,

$$\begin{aligned}\frac{1}{T}\sum_{t=1}^{T}\mathbb{E}\left[\|\boldsymbol{m}_t - \nabla F(\boldsymbol{x}_t)\|_2\right] \leq & \underbrace{\frac{1}{T}\sum_{t=1}^{T}\beta_1^t \|\nabla F(\boldsymbol{x}_1)\|_2}_{\mathcal{T}_1} + \underbrace{\frac{1-\beta_1}{T}\sum_{t=1}^{T}\mathbb{E}\left[\left\|\sum_{k=1}^{t}\beta_1^{t-k}(\boldsymbol{g}_k - \nabla F(\boldsymbol{x}_k))\right\|_2\right]}_{\mathcal{T}_2} \\ & + \underbrace{\frac{1}{T}\sum_{t=1}^{T}\mathbb{E}\left[\left\|\sum_{k=1}^{t}\beta_1^{t-k+1}(\nabla F(\boldsymbol{x}_k) - \nabla F(\boldsymbol{x}_{k-1}))\right\|_2\right]}_{\mathcal{T}_3}\end{aligned} \tag{42}$$

In terms of $\mathcal{T}_1$, we obtain

$$\mathcal{T}_1 = \frac{1}{T}\sum_{t=1}^{T}\beta_1^t \|\nabla F(\boldsymbol{x}_1)\|_2 \leq \frac{\|\nabla F(\boldsymbol{x}_1)\|_2}{T(1-\beta_1)}. \tag{43}$$

As for $\mathcal{T}_2$, we have

$$
\begin{aligned}
\mathcal{T}_2 =& \frac{1-\beta_1}{T}\sum_{t=1}^{T}\mathbb{E}\left[\left\|\sum_{k=1}^{t}\beta_1^{t-k}(\boldsymbol{g}_k-\nabla F(\boldsymbol{x}_k))\right\|_2\right] \\
\overset{(i)}{\leq}& \frac{1-\beta_1}{T}\sum_{t=1}^{T}\sqrt{\mathbb{E}\left[\left\|\sum_{k=1}^{t}\beta_1^{t-k}(\boldsymbol{g}_k-\nabla F(\boldsymbol{x}_k))\right\|_2^2\right]} \\
\overset{(ii)}{=}& \frac{1-\beta_1}{T}\sum_{t=1}^{T}\sqrt{\sum_{k=1}^{t}\beta_1^{2(t-k)}\mathbb{E}\left[\|\boldsymbol{g}_k-\nabla F(\boldsymbol{x}_k)\|_2^2\right]} \\
\overset{(iii)}{\leq}& \frac{1-\beta_1}{T}\sum_{t=1}^{T}\sqrt{\sum_{k=1}^{t}\beta_1^{2(t-k)}(\sigma_0^2+\sigma_1^2\mathbb{E}[\|\nabla F(x_k)\|_2^p])} \\
\overset{(iv)}{\leq}& \frac{1-\beta_1}{T}\sum_{t=1}^{T}\sqrt{\sum_{k=1}^{t}\beta_1^{2(t-k)}\sigma_0^2}+\frac{1-\beta_1}{T}\sum_{t=1}^{T}\sqrt{\sum_{k=1}^{t}\beta_1^{2(t-k)}\sigma_1^2\mathbb{E}[\|\nabla F(x_k)\|_2^p]} \\
\overset{(v)}{\leq}& \frac{1-\beta_1}{T}\sum_{t=1}^{T}\sqrt{\sum_{k=1}^{t}\beta_1^{2(t-k)}\sigma_0^2}+\frac{1-\beta_1}{T}\sum_{t=1}^{T}\sqrt{\sum_{k=1}^{t}\beta_1^{2(t-k)}\sigma_1^2\left(\frac{2-p}{2}+\frac{p}{2}\mathbb{E}[\|\nabla F(x_k)\|_2^2]\right)} \\
\overset{(vi)}{\leq}& \frac{1-\beta_1}{T}\sum_{t=1}^{T}\sqrt{\sum_{k=1}^{t}\beta_1^{2(t-k)}\sigma_0^2}+\frac{1-\beta_1}{T}\sum_{t=1}^{T}\sqrt{\sum_{k=1}^{t}\frac{(2-p)\sigma_1^2}{2}\beta_1^{2(t-k)}} \\
&+\frac{1-\beta_1}{T}\sum_{t=1}^{T}\sqrt{\sum_{k=1}^{t}\frac{p}{2}\beta_1^{2(t-k)}\sigma_1^2\mathbb{E}[\|\nabla F(x_k)\|_2^2]} \\
\overset{(vii)}{\leq}& \frac{1-\beta_1}{\sqrt{1-\beta_1^2}}\left(\sigma_0+\sqrt{\frac{2-p}{2}}\sigma_1\right)+\frac{1-\beta_1}{T}\sum_{t=1}^{T}\sqrt{\sum_{k=1}^{t}\frac{p\sigma_1^2}{2}\beta_1^{2(t-k)}\mathbb{E}[\|\nabla F(x_k)\|_2^2]} \\
\overset{(viii)}{\leq}& \frac{1-\beta_1}{\sqrt{1-\beta_1^2}}\left(\sigma_0+\sqrt{\frac{2-p}{2}}\sigma_1\right)+(1-\beta_1)\sqrt{\frac{1}{T}\sum_{t=1}^{T}\sum_{k=1}^{t}\frac{p\sigma_1^2}{2}\beta_1^{2(t-k)}\mathbb{E}[\|\nabla F(x_k)\|_2^2]} \\
\overset{(ix)}{\leq}& \frac{1-\beta_1}{\sqrt{1-\beta_1^2}}\left(\sigma_0+\sqrt{\frac{2-p}{2}}\sigma_1\right)+(1-\beta_1)\sqrt{\frac{p\sigma_1^2}{2}\cdot\frac{1}{T}\sum_{t=1}^{T}\mathbb{E}[\|\nabla F(x_k)\|_2^2]\sum_{k=t}^{T}\beta_1^{2(t-k)}} \\
\leq& \frac{1-\beta_1}{\sqrt{1-\beta_1^2}}\left(\sigma_0+\sqrt{\frac{2-p}{2}}\sigma_1\right)+\frac{\sqrt{p}\sigma_1(1-\beta_1)}{\sqrt{2(1-\beta_1^2)}}\sqrt{\frac{1}{T}\sum_{t=1}^{T}\mathbb{E}[\|\nabla F(x_k)\|_2^2]} \\
\overset{(x)}{\leq}& \frac{1-\beta_1}{\sqrt{1-\beta_1^2}}\left(\sigma_0+\sqrt{\frac{2-p}{2}}\sigma_1\right)+\frac{C_0\sqrt{p}\sigma_1(1-\beta_1)}{\sqrt{2(1-\beta_1^2)}}\cdot\frac{1}{T}\sum_{t=1}^{T}\mathbb{E}[\|\nabla F(x_k)\|_2] \\
\leq& \sqrt{1-\beta_1}\left(\sigma_0+\sqrt{\frac{2-p}{2}}\sigma_1\right)+C_0\sigma_1\sqrt{p(1-\beta_1)}\cdot\frac{1}{T}\sum_{t=1}^{T}\mathbb{E}[\|\nabla F(x_t)\|_2]
\end{aligned}
\tag{44}
$$

where (i) holds due to the fact $(\mathbb{E}[Z])^2 \leq \mathbb{E}[Z^2]$; (ii) holds owing to $\mathbb{E}[\boldsymbol{g}_k - \nabla F(\boldsymbol{x}_k)] = \mathbf{0}$ according to Assumption C.3; (iii) holds resulting from $\mathbb{E}\left[\|\boldsymbol{g}_k - \nabla F(\boldsymbol{x}_k)\|_2^2\right] \leq \sigma_0^2 + \sigma_1 \|\nabla F(\boldsymbol{x}_k)\|_2^p$ according to Assumption C.3; (iv) holds due to the fact $\sqrt{a+b} \leq \sqrt{a} + \sqrt{b}$; (v) holds resulting from the fact that $a^p \leq \frac{2-p}{2} + \frac{p}{2}a^2, 0 \leq p \leq 2$ according to Young's inequality; (vi) holds due to using the fact $\sqrt{a+b} \leq \sqrt{a} + \sqrt{b}$ again;(vii) holds due to the fact $\sum_i^T a_i \leq \sqrt{T}\sqrt{\sum_i^T a_i^2}$ according to Cauchy-Schwaz inequality; $(viii)$ holds owing to $\sum_{k=1}^t \beta_1^{2(t-k)} \leq \frac{1}{1-\beta_1^2}$; (ix) holds thanks to the fact $\sum_{i=1}^n \sum_{j=1}^i f(i,j)g(j) = \sum_{j=1}^n g(j) \sum_{i=j}^n f(i,j)$; (x) holds because of Condition 1.

Now we turn attention to $\mathcal{T}_3$, *i.e.*,

$$
\begin{aligned}
\mathcal{T}_3 =& \frac{1}{T}\sum_{t=1}^T \mathbb{E}\left[\left\|\sum_{k=1}^t \beta_1^{t-k+1}(\nabla F(\boldsymbol{x}_k) - \nabla F(\boldsymbol{x}_{k-1}))\right\|_2\right] \\
\overset{(i)}{\leq}& \frac{1}{T}\sum_{t=1}^T \sum_{k=1}^t \beta_1^{t-k+1}\mathbb{E}\left[\|\nabla F(\boldsymbol{x}_k) - \nabla F(\boldsymbol{x}_{k-1})\|_2\right] \\
\overset{(ii)}{\leq}& \frac{1}{T}\sum_{t=1}^T \sum_{k=1}^t \beta_1^{t-k+1}\mathbb{E}\left[(L_0 + L_1\|\nabla F(\boldsymbol{x}_k)\|_2^q)\|\boldsymbol{x}_k - \boldsymbol{x}_{k-1}\|_2\right] \\
\overset{(iii)}{=}& \frac{1}{T}\sum_{t=1}^T \sum_{k=1}^t \beta_1^{t-k+1}\mathbb{E}\left[\gamma(L_0 + L_1\|\nabla F(\boldsymbol{x}_k)\|_2^q)\|\boldsymbol{u}_{t-1}\|_2]\right) \\
\overset{(iv)}{\leq}& \frac{1}{T}\sum_{t=1}^T L_0\gamma R\sqrt{d}\sum_{k=1}^t \beta_1^{t-k+1} + \frac{L_1\gamma R\sqrt{d}}{T}\sum_{k=1}^t \beta_1^{t-k+1}\mathbb{E}[\|\nabla F(\boldsymbol{x}_k\|_2^q)] \\
\leq& \frac{\gamma L_0 R\sqrt{d}}{1-\beta} + \frac{\gamma L_1 R\sqrt{d}}{T}\sum_{t=1}^T \sum_{k=1}^t \beta_1^{t-k+1}((1-q) + q\mathbb{E}[\|\nabla F(\boldsymbol{x}_k)\|_2]) \\
\overset{(v)}{\leq}& \frac{\gamma(L_0 + (1-q)L_1)R\sqrt{d}}{1-\beta_1} + \frac{\gamma q L_1 R\sqrt{d}}{T}\sum_{t=1}^T \sum_{k=1}^t \beta_1^{t-k+1}\mathbb{E}[\|\nabla F(\boldsymbol{x}_k)\|_2] \\
\overset{(vi)}{=}& \frac{\gamma(L_0 + (1-q)L_1)R\sqrt{d}}{1-\beta_1} + \frac{\gamma q L_1 R\sqrt{d}}{T}\sum_{k=1}^T \mathbb{E}[\|\nabla F(\boldsymbol{x}_k)\|_2]\sum_{t=k}^T \beta_1^{t-k+1} \\
\leq& \frac{\gamma(L_0 + (1-q)L_1)R\sqrt{d}}{1-\beta_1} + \frac{\gamma q L_1 R\sqrt{d}}{(1-\beta_1)T}\sum_{t=1}^T \mathbb{E}[\|\nabla F(\boldsymbol{x}_t)\|_2]
\end{aligned}
\tag{45}
$$

where (i) holds due to the fact $\|\boldsymbol{a} + \boldsymbol{b}\|_2 \leq \|\boldsymbol{a}\|_2 + \|\boldsymbol{b}\|_2$; (ii) holds owing to Assumption B.3; (iii) holds due to the update rule; (iv) holds depending on $\boldsymbol{u}^{(j)} \leq {}^{1-\beta_1}/_{\sqrt{1-\beta_2}}\sqrt{1 - \frac{\beta_1^2}{\beta_2}} = R$ according to Lemma 2; (v) holds thanks to the fact that $a^q \leq (1-q) + qa$ according to Young's inequality; (vi) holds resulting from the fact that $\sum_{i=1}^n \sum_{j=1}^i \boldsymbol{a}_{i,j} = \sum_{j=1}^n \sum_{i=j}^n \boldsymbol{a}_{i,j}$.

Combining Eq.(42) - Eq.(45), we have

$$\begin{aligned}\frac{1}{T}\sum_{t=1}^{T}\mathbb{E}\left[\|\boldsymbol{m}_t-\nabla F(\boldsymbol{x}_t)\|_2\right]\leq&\frac{\|\nabla F(\boldsymbol{x}_1)\|_2}{T(1-\beta_1)}+\sqrt{1-\beta_1}\left(\sigma_0+\sqrt{\frac{2-p}{2}}\sigma_1\right)\\&+C_0\sigma_1\sqrt{p(1-\beta_1)}\cdot\frac{1}{T}\sum_{t=1}^{T}\mathbb{E}\left[\|\nabla F(x_t)\|_2\right]\\&+\frac{\gamma R\sqrt{d}(L_0+(1-q)L_1)}{1-\beta_1}+\frac{\gamma R\sqrt{d}qL_1}{1-\beta_1}\cdot\frac{1}{T}\sum_{t=1}^{T}\mathbb{E}[\|\nabla F(\boldsymbol{x}_t)\|_2]\end{aligned}\tag{46}$$

Combining Eq.(39) and Eq.(46), we obtain

$$\begin{aligned}&\frac{1}{T}\left(\sum_{t=1}^{T}\mathbb{E}[\|\boldsymbol{u}_t\circ\nabla F(\boldsymbol{x}_t)\|_1]-\left(\frac{\gamma R^2dqL_1}{2}+2C_0R\sqrt{d}\sigma_1\sqrt{p(1-\beta_1)}+\frac{2\gamma R^2dqL_1}{1-\beta_1}\right)\sum_{t=1}^{T}\mathbb{E}[\|\nabla F(\boldsymbol{x}_t)\|_2]\right)\\\leq&\frac{F(\boldsymbol{x}_1)-F^*}{\gamma T}+\frac{2R\sqrt{d}\,\|\nabla F(\boldsymbol{x}_1)\|_2}{T(1-\beta_1)}+2R\sqrt{d}\sqrt{1-\beta_1}\left(\sigma_0+\sqrt{\frac{2-p}{2}}\sigma_1\right)\\&+\frac{2\gamma R^2d(L_0+(1-q)L_1)}{1-\beta_1}+\frac{\gamma R^2d(L_0+(1-q)L_1)}{2}.\end{aligned}\tag{47}$$

B.4 Proof of Corollary 3

Proof. (1) Choosing $\bar{v}=\min_t\mathbb{E}[\boldsymbol{u}_t^{(j)}]$, we have

$$\begin{aligned}\sum_{t=1}^{T}\mathbb{E}[\|\boldsymbol{u}_t\circ\nabla F(\boldsymbol{x}_t)\|_1]=&\sum_{t=1}^{T}\sum_{j=1}^{d}\mathbb{E}[|\boldsymbol{u}_t^{(j)}\nabla F(\boldsymbol{x}_t^{(j)})|]\\\overset{(i)}{=}&\sum_{t=1}^{T}\sum_{j=1}^{d}\mathbb{E}[\boldsymbol{u}_t^{(j)}]\mathbb{E}[|\nabla F(\boldsymbol{x}_t^{(j)})|]\\\overset{(ii)}{=}&\sum_{t=1}^{T}\mathbb{E}[\boldsymbol{u}_t^{(j)}]\sum_{j=1}^{d}\mathbb{E}[|\nabla F(\boldsymbol{x}_t^{(j)})|]\\=&\sum_{t=1}^{T}\mathbb{E}[\boldsymbol{u}_t^{(j)}]\mathbb{E}[\|(\nabla F(\boldsymbol{x}_t))\|_1]\\\overset{(iii)}{\geq}&\bar{v}\sum_{t=1}^{T}\mathbb{E}[\|(\nabla F(\boldsymbol{x}_t))\|_1]\\\overset{(iv)}{=}&\frac{\bar{v}\sqrt{d}}{C_1}\sum_{t=1}^{T}\mathbb{E}[\|(\nabla F(\boldsymbol{x}_t))\|_2],\end{aligned}\tag{48}$$

where (i) holds due to $\boldsymbol{u}_t^{(j)}$ and $|\nabla F(\boldsymbol{x}_t^j)|$ are mutually independent; (ii) holds owing to applying Condition 2; (iii) holds due to the condition $\bar{v}\leq\min_t\mathbb{E}[\boldsymbol{u}_t^{(j)}]$; (iv) holds depending on Condition 3.

Then, we simplify the conclusion in Theorem 2 as

$$\begin{aligned}&\left(\bar{v}-\left(\frac{\gamma C_1 R^2\sqrt{d}qL_1}{2}+2C_0C_1R\sigma_1\sqrt{p(1-\beta_1)}+\frac{2\gamma C_1R^2\sqrt{d}qL_1}{1-\beta_1}\right)\right)\cdot\frac{1}{T}\sum_{t=1}^{T}\mathbb{E}[\|\nabla F(\boldsymbol{x}_t)\|_2]\\ \leq&\frac{C_1(F(\boldsymbol{x}_1)-F^*)}{\gamma T\sqrt{d}}+\frac{2C_1R\left\|\nabla F(\boldsymbol{x}_1)\right\|_2}{T(1-\beta_1)}+2C_1\sqrt{1-\beta_1}R\hat{\sigma}+\frac{2\gamma C_1R^2\sqrt{d}\hat{L}}{1-\beta_1}+\frac{\gamma C_1R^2\sqrt{d}\hat{L}}{2}.\end{aligned}\tag{49}$$

Choosing $\gamma=\frac{C_2}{T^{3/4}d^{1/2}}$, $1-\beta_1=\frac{C_3}{T^{1/2}}$ and $T\geq(\frac{4C_1C_2R^2qL_1}{C_3\bar{v}}+\frac{4C_0C_1\sqrt{C_3}R\sigma_1\sqrt{p}}{\bar{v}}+(\frac{C_1C_2R^2qL_1}{\bar{v}})^{1/3})^4$, following Lemma 4, it holds that

$$\frac{\gamma C_1R^2\sqrt{d}qL_1}{2}+2C_0C_1R\sigma_1\sqrt{p(1-\beta_1)}+\frac{2\gamma C_1R^2\sqrt{d}qL_1}{1-\beta_1}\leq\frac{\bar{v}}{2}.\tag{50}$$

Then, we reformulate Eq. (49) as

$$\frac{1}{T}\sum_{t=1}^{T}\mathbb{E}[\|\nabla F(\boldsymbol{x}_t)\|_2]\leq\frac{C_1}{\bar{v}}\left(\frac{2(F(\boldsymbol{x}_1)-F(\boldsymbol{x}^*))}{C_2T^{1/4}}+\frac{4R\left\|\nabla F(\boldsymbol{x}_1)\right\|_2}{C_3T^{1/2}}+\frac{4C_3R\hat{\sigma}}{T^{1/4}}+\frac{4C_2R^2\hat{L}}{C_3T^{1/4}}+\frac{C_2R^2\hat{L}}{T^{3/4}}\right).\tag{51}$$

(2) Using generalized Young's inequality, we minimize the bottle-neck terms to obtain the lowerest bound on the right hand of Eq. (49), *i.e.*,

$$\begin{aligned}&\frac{C_1(F(\boldsymbol{x}_1)-F^*)}{\gamma T\sqrt{d}}+2C_1\sqrt{1-\beta_1}R\hat{\sigma}+\frac{2C_1\gamma R^2\sqrt{d}\hat{L}}{1-\beta_1}\\ \geq&\left(\frac{4C_1(F(\boldsymbol{x}_1)-F^*)}{\gamma T\sqrt{d}}\right)^{1/4}\cdot\left(4C_1\sqrt{1-\beta_1}R\hat{\sigma}\right)^{1/2}\cdot\left(\frac{8C_1\gamma R^2\sqrt{d}\hat{L}}{1-\beta_1}\right)^{1/4}\\ =&\frac{512^{1/4}C_1R\hat{\sigma}^{1/2}\hat{L}^{1/4}(F(\boldsymbol{x}_1)-F^*)^{1/4}}{T^{1/4}},\end{aligned}\tag{52}$$

where the lowest bound achieved if and only if $\frac{4C_1(F(\boldsymbol{x}_1)-F^*)}{\gamma T\sqrt{d}}=4C_1\sqrt{1-\beta_1}R\hat{\sigma}$ and $4C_1\sqrt{1-\beta_1}R\hat{\sigma}=\frac{8C_1\gamma R^2\sqrt{d}\hat{L}}{1-\beta_1}$, and we further obtain

$$\begin{aligned}\gamma&=\frac{(F(\boldsymbol{x}_1)-F^*)^{3/4}}{2^{1/4}T^{3/4}d^{1/2}R\hat{\sigma}^{1/2}\hat{L}^{1/4}},\\ \beta_1&=1-\frac{2^{1/2}\hat{L}^{1/2}(F(\boldsymbol{x}_1)-F^*)^{1/2}}{T^{1/2}\hat{\sigma}}.\end{aligned}\tag{53}$$

When it is chosen $T\geq(\frac{4C_1\hat{C}_2R^2qL_1}{\hat{C}_3\bar{v}}+\frac{4C_0C_1\sqrt{\hat{C}_3}R\sigma_1\sqrt{p}}{\bar{v}}+(\frac{C_1\hat{C}_2R^2qL_1}{\bar{v}})^{1/3})^4$ where $\hat{C}_2=\frac{(F(\boldsymbol{x}_1)-F^*)^{3/4}}{2^{1/4}R\hat{\sigma}^{1/2}\hat{L}^{1/4}}$ and $C_3=\frac{2^{1/2}\hat{L}^{1/2}(F(\boldsymbol{x}_1)-F^*)^{1/2}}{\hat{\sigma}}$, following Lemma 4, it holds that

$$\frac{\gamma C_1R^2\sqrt{d}qL_1}{2}+2C_0C_1R\sigma_1\sqrt{p(1-\beta_1)}+\frac{2\gamma C_1R^2\sqrt{d}qL_1}{1-\beta_1}\leq\frac{v}{2}.\tag{54}$$

Then, we reformulate Eq. (49) as

$$\frac{1}{T}\sum_{t=1}^{T}\mathbb{E}[\|\nabla F(\boldsymbol{x}_t)\|_2] \leq \frac{C_1}{\bar{v}}\left(\frac{512^{1/4}R\hat{\sigma}^{1/2}\hat{L}^{1/4}(F(\boldsymbol{x}_1)-F^*)^{1/4}}{T^{1/4}} + \frac{4R\|\nabla F(\boldsymbol{x}_1)\|_2}{\hat{C}_3T^{1/2}} + \frac{\hat{C}_2R^2\hat{L}}{T^{3/4}}\right). \tag{55}$$

B.5 Convergence of Adam without Condition 1-3

In the proof of Lemma 2, Condition 1 is no longer necessary when Assumption C.1 is used. Even in the absence of Conditions 1, 2, and 3, and assuming no access to the oracle values L_0, L_1, σ_0, and σ_1, we can still theoretically establish that $\frac{1}{T}\sum_{t=0}^{T-1}\mathbb{E}[\|\nabla F(\boldsymbol{x}_t)\|_2]$ for Adam converges at the rate of $O\left(\frac{1}{T^{1/4}}\right)$, under the assumptions of (L_0, L_1, q)-smoothness and affine variance.

Theorem 4 (Convergence of Adam without Condition 1-3) *Let $\{x_t\}_{t=0}^{T-1}$ be generated by Algorithm 1. Suppose that Assumptions A, B.3 and C.1 hold. Define $u_t^{(j)} := |\boldsymbol{m}_t^{(j)}|/(\sqrt{\boldsymbol{v}_t^{(j)}}+\epsilon)$, $R := 1-\beta_1/\sqrt{(1-\beta_2)(1-\beta_1^2/\beta_2)}$ and $\hat{L} := L_0+(1-q)L_1$. Choose $\gamma = \frac{C_2}{T^{3/4}d^{1/2}}$, $\beta_1 < \sqrt{\beta_2}$, $1-\beta_1 = \frac{C_3}{T^{1/2}}$ and $0 < v \leq \min_{t,j} u_t^{(j)}$. Then, it holds for any $T \in \mathbb{N}^+$ and $T \geq (\frac{4C_2R^2d^{1/2}qL_1}{C_3v} + (\frac{C_2R^2d^{1/2}qL_1}{v})^{1/3})^4$,*

$$\frac{1}{T}\sum_{t=0}^{T-1}\mathbb{E}[\|\nabla F(\boldsymbol{x}_t)\|_1] \leq \frac{1}{v}\left(\frac{2(F(\boldsymbol{x}_0)-F(\boldsymbol{x}^*))}{C_2T^{1/4}d^{1/2}} + \frac{4Rd^{1/2}\|\nabla F(\boldsymbol{x}_0)\|_2}{C_3T^{1/2}} + \frac{4C_3Rd^{1/2}\sigma_0}{T^{1/4}} + \frac{4C_2R^2d^{1/2}\hat{L}}{C_3T^{1/4}} + \frac{C_2R^2d^{1/2}\hat{L}}{T^{7/4}}\right). \tag{56}$$

Proof. When C.1 holds, it implies $\sigma_1 = 0$. Also, it is known that $\|\nabla F(\boldsymbol{x}_t)\|_2 \leq \|\nabla F(\boldsymbol{x}_t)\|_1$. Hence, the conclusion in Theorem 2 can be simplified as

$$\left(v - \frac{\gamma R^2dqL_1}{2} - \frac{2\gamma R^2dqL_1}{1-\beta_1}\right)\cdot\frac{1}{T}\sum_{t=1}^{T}\mathbb{E}[\|\nabla F(\boldsymbol{x}_t)\|_1] \leq \frac{F(\boldsymbol{x}_1)-F^*}{\gamma T} + \frac{2R\sqrt{d}\|\nabla F(\boldsymbol{x}_1)\|_2}{T(1-\beta_1)} + 2\sqrt{1-\beta_1}R\sqrt{d}\sigma_0 + \frac{2\gamma R^2d\hat{L}}{1-\beta_1} + \frac{\gamma R^2d\hat{L}}{2}, \tag{57}$$

where $0 < v \leq \min_{t,j} \boldsymbol{u}_t^{(j)}$ and $\hat{L} = L_0 + (1-q)L_1$.

Choosing $\gamma = \frac{C_2}{T^{3/4}d^{1/2}}$ and $1-\beta_1 = \frac{C_3}{T^{1/2}}$ and $T \geq (\frac{4C_2R^2d^{1/2}qL_1}{C_3v} + (\frac{C_2R^2d^{1/2}qL_1}{v})^{1/3})^4$, following Lemma 4, it holds that

$$\frac{\gamma R^2dqL_1}{2} + \frac{2\gamma R^2dqL_1}{1-\beta_1} \leq \frac{v}{2}. \tag{58}$$

Then, we arrive the conclusion

$$\frac{1}{T}\sum_{t=1}^{T}\mathbb{E}[\|\nabla F(\boldsymbol{x}_t)\|_1] \leq \frac{1}{v}\left(\frac{2d^{1/2}(F(\boldsymbol{x}_1)-F(\boldsymbol{x}^*))}{C_2T^{1/4}} + \frac{4Rd^{1/2}\|\nabla F(\boldsymbol{x}_1)\|_2}{C_3T^{1/2}} + \frac{4C_3Rd^{1/2}\sigma_0}{T^{1/4}} + \frac{4C_2R^2d^{1/2}\hat{L}}{C_3T^{1/4}} + \frac{C_2R^2d^{1/2}\hat{L}}{T^{3/4}}\right). \tag{59}$$